

STUDY OF AIR FLOW IN A ROOM WITH AND WITHOUT WALL TEMPERATURE DIFFERENTIALS

A DISSERTATION

Submitted in partial fulfilment of the
requirements for the award of the degree

of

MASTER OF TECHNOLOGY

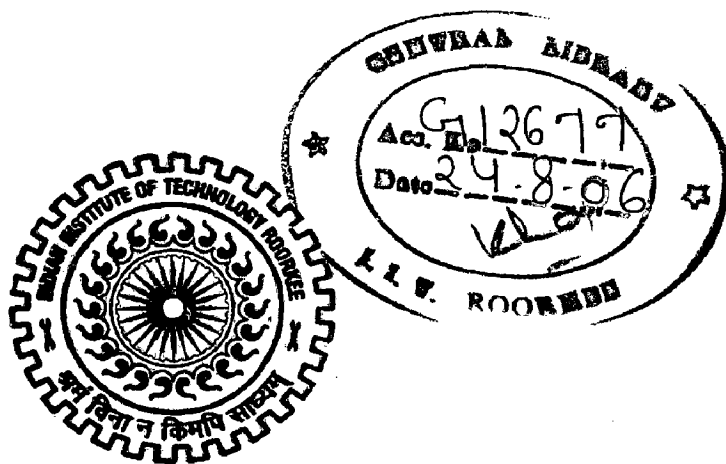
in

CHEMICAL ENGINEERING

(With Specialization in Industrial Safety and Hazards Management)

By

RAVICHAND KAKUMANU



DEPARTMENT OF CHEMICAL ENGINEERING
INDIAN INSTITUTE OF TECHNOLOGY ROORKEE
ROORKEE-247 667 (INDIA)

JUNE, 2006

Candidate's declaration

I hereby declare that the work, which is being presented in the dissertation, entitled, **“STUDY OF AIR FLOW IN A ROOM WITH AND WITHOUT WALL TEMPERATURE DIFFERENTIALS”** submitted in partial fulfillment of the requirements for the award of degree of **Master of Technology** in Chemical Engineering with specialization in **“INDUSTRIAL SAFETY AND HAZARDS MANAGEMENT”** submitted in the Department of **CHEMICAL ENGINEERING**, Indian Institute of Technology, Roorkee, India, is an authentic record of my own work carried out under the supervision of **Dr.R.BHARGAVA**, Asst.professor, Department of Chemical Engineering, IIT Roorkee and **Sri P.K.BHARGAVA**, Scientist F, Central Building research Institute.

The matter embodied in this dissertation has not been submitted by me for the award of any other degree.

Date: 28-06-2006

Place: Roorkee

K. Ravichand
(RAVICHAND KAKUMANU)


Certificate

This is to certify that above statement made by candidate is correct to best of my knowledge and belief.

 28/6/06

Sri P.K.BHARGAVA

Central Building research Institute,
Scientist F.

 28.6.06

Dr.R.BHARGAVA

Asst.professor,
Department of Chemical Engineering,
IIT Roorkee.

Acknowledgement

I wish to express my deep sense of gratitude and sincere thanks to my loving guide **Dr. R. BHARGAVA**, Asst. professor, Department of Chemical Engineering, IIT Roorkee and **Sri P. K. BHARGAVA**, Scientist F, Central Building Research Institute, for their valuable guidance. This work is simply the reflection of their thoughts, ideas, and concepts and above all, their efforts. I am highly indebted to them for their kind and valuable suggestions and of course his valuable time during the period of the work. The huge quantum of knowledge, had gained during their inspiring guidance would me immensely beneficial for my future endeavors.

I express my sincere thanks to Dr. BIKASH MOHANTY, professor for providing manuals about CFD packages. I am also thankful to Dr. SHRICHAND, Head of the Department, Chemical Engineering Department and other staff members for their instant help in all kinds of work. I extend warm appreciation to all of my friends for their continuous support and enthusiastic help.

K. Ravichand
(RAVICHAND KAKUMANU)

ABSTRACT

Accurate prediction of velocity and temperature distributions in a room is indispensable for designing high quality air conditioning systems. This dissertation work is concerned with the feasibility and validity of numerical simulation of room air flow. Turbulent recirculating flows in many types of ventilated rooms were numerically simulated in three-dimensions using the $k-\varepsilon$ two equation turbulence model. Since 3-D simulation requires a large amount of computer storage and computational time it was impossible in the past to conduct such types of simulations with sufficient accuracy due to limitations of computer resources. However, recent advances in computer technology and in numerical methods for fluid dynamics now make it possible to conduct such large scale simulations.

In this study the air flow in a small scale room is simulated numerically using two different turbulent models those are $k-\varepsilon$ two equation model and Large Eddy Simulation. The air flow patterns are very complicated since heat and momentum sources are distributed. The supply air devices can not be described in detail without the computational grid becoming impractically large. Therefore, an integral part of a CFD simulation is to simplify the actual flow situation without losing essential features of the flow. In this study two different room models are considered. Room is cubical in shape and has one inlet and two outlets. In one model wall temperature differentials are considered whereas in the other one wall temperatures are constant. For both cases the vector plots of velocity and contour plots of air velocity are studied. For the wall temperature differential model the temperature profiles are studied.

CONTENTS

	TITLE	PAGE NO
CHAPTER 1	INTRODUCTION	1
	1.1 General introduction	1
	1.2 Problem statement	3
CHAPTER 2	LITERATURE REVIEW	5
	2.1 Computational fluid dynamics	5
	2.1.1 Applications of CFD	6
	2.1.2 Mathematics of CFD	10
	2.2 Fluid dynamics theory	10
	2.2.1 Laminar flow equations	11
	2.2.1.1 Conservation of mass and momentum	11
	2.2.1.2 Energy equation	11
	2.2.2 Turbulent flow equations	11
	2.2.2.1 Mean value approach to turbulence	11
	2.2.2.2 Turbulent Flow Equations – Continuity	13
	2.2.2.3 Turbulent Flow Equations – Momentum	13
	2.2.3 Turbulence modeling theory	14

	2.2.3.1	k- ε Turbulence Model	16
	2.2.3.2	Low reynolds number model	18
	2.2.3.3	Large Eddy Simulation	21
	2.3	Other models	22
CHAPTER 3		MODEL AND MODEL EQUATIONS	31
	3.1	Mathematical model	31
	3.1.1	Continuity equation	31
	3.1.2	Momentum equation	31
	3.1.3	Transport equation for k	32
	3.1.4	Transport equation for ε	32
	3.2	Boundary conditions	33
	3.2.1	Inlet conditions	33
	3.2.2	Outlet conditions	34
	3.2.3	Wall boundary	34
CHAPTER 4		NUMERICAL SIMULATION TECHNIQUE	35
	4.1	Development of geometric model 1	35
	4.2	Mesh generation of model 1	37
	4.3	Solution process of model 1	39
	4.4	Development of geometric model 2	42
	4.5	Mesh generation of model 2	43
	4.6	Solution process of model 2	46

CHAPTER 5	RESULTS AND DISCUSSIONS	48
5.1	Model 1 results	48
5.1.1	Results from k- ε modell	48
5.1.2	Results from Large Eddy simulation	53
5.2	Model 2 results	56
CHAPTER 6	CONCLUSIONS AND RECOMMENDATIONS	64
	NOMENCLATURE	66
	REFERENCES	68

LIST OF FIGURES

Table no.	Description	page no
Fig.2.1	Tree of turbulence modeling	15
Fig.2.2	Experimental facility [Spitler 1990]	24
Fig.4.1	Representation of a model 1 in Top view	35
Fig.4.2	Representation of a model 1 in side view	36
Fig.4.3	Representation of a model 1 in Isometric view	36
Fig.4.4	Meshing geometry of model 1	38
Fig.4.5	Labeled geometry of model 1	39
Fig.4.6	Representation of a model 2 in Isometric view	43
Fig.4.7	Meshing geometry of model 2	45
Fig.4.8	Labeled geometry of model 2	45
Fig.5.1	Convergence history of static pressure on boundary_type	48
Fig.5.2	Scaled residuals	49
Fig.5.3	Grid display	49
Fig.5.4	Velocity vectors colored by velocity magnitude (m/s)	50
Fig.5.5	Velocity vectors colored by velocity magnitude at x=1m	50
Fig.5.6	Velocity vectors colored by velocity magnitude at x=3m	51
Fig.5.7	Velocity vectors colored by velocity magnitude at x=4m	51
Fig.5.8	Velocity vectors colored by velocity magnitude at x=5m	51
Fig.5.9	Contours of velocity magnitude (m/s) at x= 1m	52

Fig.5.10	Contours of velocity magnitude (m/s) at x= 3m	52
Fig.5.11	Contours of velocity magnitude (m/s) at x=4m	53
Fig.5.12	Contours of velocity magnitude (m/s) at x= 5m	53
Fig.5.13	Convergence history of static pressure on boundary_type For LES model apply to model 1	54
Fig.5.14	Velocity vectors colored by velocity magnitude (m/s)	54
Fig.5.15	Velocity vectors colored by velocity magnitude For LES model apply to model1 at x=1m	55
Fig.5.16	Velocity vectors colored by velocity magnitude For LES model apply to model1 at x=3m	55
Fig.5.17	Velocity vectors colored by velocity magnitude For LES model apply to model1 at x=4m	55
Fig.5.18	Velocity vectors colored by velocity magnitude For LES model apply to model1 at x=5m	56
Fig.5.19	Scaled residuals for model 2	57
Fig.5.20	Convergence history of static pressure on boundary_type	57
Fig.5.21	Velocity vectors colored by velocity magnitude (m/s) For model 2	57
Fig.5.22	Contours of static temperature (k) at x=1m For model 2	58
Fig.5.23	Contours of static temperature (k) at x=3m For model 2	58
Fig.5.24	Contours of static temperature (k) at x=4m For model 2	59
Fig.5.25	Contours of static temperature (k) at x=5m For model 2	59
Fig.5.26	Velocity vectors colored by velocity magnitude at x=1m For model 2	60

Fig.5.27	Velocity vectors colored by velocity magnitude at $x=3\text{m}$ For model 2	60
Fig.5.28	Velocity vectors colored by velocity magnitude at $x=4\text{m}$ For model 2	60
Fig.5.29	Velocity vectors colored by velocity magnitude at $x=5\text{m}$ For model 2	61
Fig.5.30	Contours of velocity magnitude (m/s) at $x= 1\text{m}$ for model 2	61
Fig.5.31	Contours of velocity magnitude (m/s) at $x= 1\text{m}$ for model 2	62
Fig.5.32	Contours of velocity magnitude (m/s) at $x= 1\text{m}$ for model 2	62
Fig.5.33	Contours of velocity magnitude (m/s) at $x= 1\text{m}$ for model 2	62
Fig.5.34	Contours of velocity magnitude (m/s) at $z= 5\text{m}$ for model 2	63

LIST OF TABLES

Table no	Description	page no
Table 2.1	Constants for standard k- ε model	17
Table 2.2	Low Reynolds k- ε constants	20
Table 2.3	Low Reynolds k- ε functions	21
Table 2.4	Experimental configurations [Spitler,1990a]	23
Table 2.5	Inlet and Outlet dimensions [Spitler,1991]	25
Table 2.6	Experimental tests [Spitler,1991]	25
Table 4.1	Discretization schemes	41
Table 4.2	Convergence criterion	42

1.1 GENERAL INTRODUCTION

As the majority of people spend most of their time indoors and often share the same space, knowledge and prediction of the indoor climate conditions is important to optimize the indoor climate for the occupants at the design phase. A gamut of parameters determine the indoor climate and are important for the well-being of the occupant of a room in terms of thermal comfort and (perceived) indoor air quality. The present work has focussed on two Parameters namely velocity and temperature.

In recent year have lead to a renewed interest for personal control within a building and especially for air conditioning systems. Such systems intend to condition a small space around the occupant, controlled by the occupant. Given the focus on the occupant level, more detailed information is required on the climate within a small space around the person: the micro-climate. The air change rate and the supply and exhaust conditions at the room level (or the macro-climate) do not present sufficient information to evaluate the micro-climate. The flow pattern determines the effectiveness with which a room is ventilated and has a large influence on the local thermal conditions.

The accurate prediction of flow behavior within a room may significantly improve heating, ventilation, and air-conditioning (HVAC) design techniques. Successful predictions of room air flow yield such information as velocities, temperatures, and contaminant distributions which are useful to building design and analysis. Ventilation and indoor air quality are only two of the many areas which would benefit by the development and refinement of room air flow modeling. The nature of room air flow requires the solution of the continuity and momentum (Navier-Stokes)

equations in three dimensions. For typical room/system combinations, the flow is at least partially turbulent. Therefore, the solution process should somehow account for turbulence.

For the determination and prediction of the indoor air flow pattern two important tools are available: *measurement* and *simulation* (Computational Fluid Dynamics - CFD). Both tools currently however have limitations in accuracy and reliability with which the flow pattern can be determined.

Advanced numerical methods and algorithms for the solution of the partial differential equations governing fluid dynamics have existed for some time [Harlow, 1965;Launder, 1972]. However, the lack of sufficient computational capabilities hindered the existence of turbulent solutions which adequately modeled fluid flow in practical situations [Launder, 1974]. The overwhelming need for turbulent flow solutions has led to the development of numerous turbulent models. Coupled and uncoupled differential and algebraic equations were derived in an effort to approximate the nature of practical turbulent flows.

Recent technological advances in computing capabilities have broadened the potential for applications of numerical prediction in fluid flow. These applications are generally referred to as Computational Fluid Dynamics (CFD) and are increasingly being used to obtain solutions for problems which were previously deemed "unsolvable" due to their complexity or the lack of sufficient computing power. The goal of this investigation is to research the various modeling techniques applicable in room air flow prediction, including turbulence models beside velocity and temperature distribution with walls having temperature differentials is to be studied.

1.2 PROBLEM STATEMENT

The main objective of buildings has always been to provide shelter from sun, wind, cold and rain. In the past designs were relatively simple and took into consideration the local environmental conditions. With respect to the indoor climate, passive cooling was provided through natural ventilation and/or thermal mass and additional heating was possible. Often “builder” and “occupant” were one and the same. This meant that issues such as personal comfort were given a high priority.

At the end of the 19th century new building construction technology was introduced. This new technology and materials such as steel made it possible to design higher and deeper buildings. Artificial lighting and ventilation created an indoor climate largely independent of outdoor climate conditions. The increased technological complexity and size of modern buildings lead to specialization in the building industry. As a result buildings very often are not being built around the needs of individual occupants, but for broader functions.

Importance of indoor air flow - To date, most people spend the majority of their time indoors, often in shared spaces. With the introduction of mechanical environmental control systems, and the resulting increased control of the indoor climate, the expectations of the occupant for a thermally comfortable indoor climate have risen. The fulfilment to these expectations however is impeded by the fact that thermal comfort conditions within a building enclosure.

In addition to thermal comfort, indoor air quality (IAQ) has become a topic of concern. This problem originated in the early 1970's energy crisis, when saving energy became a priority above all other requirements. From this time on building facades were gradually better insulated and sealed to prevent air leakage. Natural or local mechanical ventilation was replaced with central mechanical ventilation. As a further measure, the air flow rate was also reduced. A centrally controlled ventilation system with a low room ventilation rate makes maintaining acceptable conditions at occupant level more difficult. Fresh air cannot be provided directly to

the occupant. Furthermore, correction of the conditions via natural ventilation (i.e. opening a window) is no longer possible because of a sealed facade.

In view of the importance of thermal comfort and indoor air quality, the design challenge is to achieve acceptable indoor environmental conditions for each individual occupant of a building. Such an approach to design is in stark contrast with the current prevailing attitude which is directed towards designing an uniform *climate* for buildings rather than *comfort* for people.

The requirements for indoor air quality and thermal comfort are counteracting. High air flow rates, as preferred for indoor air quality, may cause draught problems in the inhabited zone. An optimal indoor climate, i.e. good indoor air quality and thermal comfort for each individual occupant of a room is aimed at nevertheless. Preferably this already should be confirmed in the design phase. Given these demands, present work is focussing on:

- the emission and absorption characteristics of materials,
- thermal comfort, and
- ventilation effectiveness.

Knowledge of the indoor emission of contaminants and the diffusion of the air flow are necessary to predict the indoor air quality.

The prediction of thermal comfort with the models of Fanger has shown to be unfeasible in a large number of cases and therefore thermal comfort has remained a topic of concern since. Currently new insights and new techniques are used to improve the creation of thermally comfortable conditions to the occupant.

The effectiveness of a ventilation system is mainly determined by (a) the removal of internally produced contaminants from the room and (b) the supply of fresh air of acceptable quality in the room, in particular to the inhabited zone. The ventilation effectiveness depends on the entire air flow pattern in a room. The availability of Computational Fluid Dynamics significantly enlarged the possibilities to further investigate this topic.

2.1 Computational Fluid Dynamics (CFD):

Computational Fluid Dynamics can be summarized by the following definitions:

Computational

The computational part of CFD means using computers to solve problems in fluid dynamics. This can be compared to the other main areas of fluid dynamics, such as theoretical and experimental.

Fluid

When most people hear the term fluid they think of a liquid such as water. In technical fields, fluid actually means anything that is not solid, so that both air and water are fluids. More precisely, any substance that cannot remain at rest under a sliding or shearing stress is regarded as a fluid.

Dynamics

Dynamics is the study of objects in motion and the forces involved. The field of fluid mechanics is similar to fluid dynamics, but usually is considered to be the motion through a fluid of constant density.

This shows that CFD is the science of computing the motion of air, water, or any other gas or liquid.

The science of computational fluid dynamics is made up of many different disciplines from the fields of transport phenomenon, mathematics, and computer science. A scientist or engineer working in the CFD field is likely to be concerned with topics such as stability analysis, graphic design, and aerodynamic optimization. CFD may be structured into two parts, generating or creating a solution, and analyzing or visualizing the solution. Often the two parts overlap, and a solution is analyzed while it is in the process of being generated in order to ensure no mistakes have been made. This is often referred to as validating a CFD simulation.

2.1.1 Applications of CFD

Computational fluid dynamics CFD is a tool used for the analysis of systems involving fluid flow, heat transfer and associated phenomena such as chemical reaction by means of computer based simulation. This technique is very powerful and spans a wide range of industrial and non-industrial application areas. Some examples are:

- Aerodynamics of aircraft and vehicle : lift and drag
- Hydrodynamics of ships
- Combustion in IC engines and gas turbines
- Turbo machinery : flows inside rotating passages, diffusers etc.
- Electrical electronics engineering : cooling of equipment including micro circuits.
- Chemical process engineering : mixing and separation, polymer moulding
- External, internal environment of building : wind loading and heating/ventilation
- Environmental engineering : distribution of pollutants and effluents
- Hydrology and oceanography : flows in rivers, estuaries,oceans.
- Biomedical engineering : blood flows through arteries and veins.

From the 1960s onwards the aerospace industry has integrated CFD techniques into the design, R&D and manufacture of aircraft and jet engines. More recently the methods have been applied to the design of internal combustion engines, combustion chambers of gas turbines and furnaces. Furthermore, motor vehicle manufacturers now originally predict drag forces, under-bonnet air flows and the in car environment with CFD. Increasingly CFD is becoming a vital component in the design of industrial products and processes.

A good understanding of the numerical simulation algorithm is also crucial. Three mathematical concepts are useful in determining the success or otherwise of such algorithm : convergence, consistency and stability. Convergence is the property of a

numerical method to produce a solution which approaches the exact solution as the grid spacing control volume size or element size is reduced to zero. Consistent numerical schemes produce systems of algebraic equations which can be demonstrated to be equivalent to the original governing equations as the grid spacing tends to zero. Stability is associated with damping of errors as the numerical methods proceeds. If a technique is not stable even runoff errors in the initial data can cause wild oscillation or divergence

CFD is the art of replacing the differential equations governing the Fluid flow and heat transfer, with a set of algebraic equations at discrete points (the process is called discretization), which in turn can be solved with the aid of a digital computer to get an approximate solution. The well known discretization methods used in CFD are Finite Difference Method (FDM), Finite volume method (FVM) and Finite Element Method FDM/FVM are the most commonly used methods for CFD applications.

There are several unique advantages of CFD over experiment-based approaches to fluid and heat transfer systems design.

- Substantial reduction of lead times and cost of new designs.
- Ability to study systems where controlled experiments are difficult or impossible to perform.
- Ability to study systems under hazardous conditions at and beyond their normal performance limits e.g. safety studies and accident scenarios.

CFD is the application of numerical techniques to solve the Navier-Stokes (N-S) equations for fluid flow. The N-S equations are derived by applying the principles of conservation of mass and momentum to a control volume of fluid. When applying CFD to the indoor air quality (IAQ) and thermal comfort problem, the conservation of mass for a contaminant Species and energy for thermal responses also may be applied.

The applicability of the semi-empirical relations often is restricted. For more detailed information on the flow field the full Navier-Stokes equations and the equation for conservation of heat must be solved. This technique is applied in Computational Fluid Dynamics (CFD). In CFD the equations have been discretised in order to solve the flow field numerically. Nielsen (1974) was one of the first to apply CFD for the numerical prediction of the indoor air flow. Since then the technique has evolved and numerous results have indicated the wide-spread applicability of CFD for the simulation of an indoor air flow pattern. The developments in computer capacity have further enhanced the application of this type of simulations. CFD has become an increasingly important tool in the prediction of the stationary indoor air flow pattern. Experience however also indicates the limitations of the current available CFD-methods, with respect to, e.g., the reliability and the sensitivity, and the necessity to validate CFD-results of typical indoor air flow patterns.

To apply CFD, the geometry of interest is first divided, or discretized, into a number of computational cells. Discretization is the method of approximating the differential equations by a system of algebraic equations for the variables at some set of discrete locations in space and time. The discrete locations are referred to as the grid or mesh.

Once the grid has been created, boundary conditions need to be applied. Pressure, velocities, mass flows and scalars such as temperature may be specified at inlets; temperature, wall shear rates, or heat fluxes may be set at walls and pressure or flow rate splits may be fixed at outlets. The component material transport properties, such as density, viscosity, and heat capacity, need to be prescribed as constant or selected from a database. These can be functions of temperature, pressure or any other variable of state.

Fluids can be modeled as either incompressible or compressible. The viscosity of the fluid can be Newtonian, or non-Newtonian, using the power law or viscosity models.

With the grid created, the boundary conditions and physical properties defined, the calculations can start. The code will solve the appropriate conservation equations for all grid cells using an iterative procedure.

Special attention needs to be paid to accurate modeling of turbulence. The presence of turbulent fluctuations, which are functions of time and position, contribute a mean momentum flux or Reynolds stress for which analytical solutions are nonexistent. These Reynolds stresses govern the transport of momentum due to turbulence and described by additional terms in Reynolds-averaged Navier-Stokes equations. The purpose of a turbulence model is to provide numerical values for the Reynolds stresses as realistically as possible, while maintaining a low level of complexity. When modeling chemical reactors using CFD, the fluid flow pattern and temperature field are calculated from conservation equations for mass, momentum and enthalpy.

The turbulence model chosen should be best suited to the particular flow problem. A wide range of models is available, and understanding the limitations and advantages of the selected one is required if the best answer is to be obtained with the minimum computation. The type of model that is chosen must be done so with care.

With the advent of high performance computers and rapid growth in CFD, it is now possible to simulate fluid flow and heat transfer in a wide range of process designs because of improvements in computer power and enhanced graphics softwares, it is now much easier for CFD analyst to create animations of their data. These often help in understanding complex flow phenomenon that are some times difficult to see from static plots. In the past, CFD was the realm of high powered computer systems. But, much of today's modeling work can be accomplished on low end UNIX work stations or high end PCs. This technique can be used to complement physical modeling. Some design engineers actually use it to analyze new systems before deciding which and how many validation tests need to be performed.

There are a number of different CFD codes available such as CFX, FLUENT, FLOW3D, ASTEC, PHOENICS, FIDAP etc..

In short we can say that Computational Fluid Dynamics (CFD) is a computer based tool for simulating the behavior of systems involving fluid flow, heat transfer and other related physical processes. It works by solving the equations of fluid flow (in a special form) over a region of interest, with specified (known) conditions on the boundary of that region.

2.1.2 The mathematics of CFD

The set of equations which describe the processes of momentum, heat and mass transfer are known as the Navier-stokes equations. These are partial differential equations which were derived in nineteenth century. They have no known general analytical solution but can be discretised and solved numerically. Equations describing other processes, such as reaction combustion etc., can also be solved in conjunction with the Navier-stokes equations. Often, an approximating model is used to derive these additional equations, turbulence models being a particularly important example.

There are a number of different solution methods which are used in CFD codes. The most common is known as the finite volume technique.

In this technique, the region of interest is divided into small sub regions, called control volumes. The equations are discretised and solved iteratively for each control volume. As a result, an approximation of the value of each variable at specific points throughout the domain can be obtained. In this way one derives a full picture of the behavior of the flow.

2.2 FLUID DYNAMICS THEORY

This section details the basic fluid dynamic principles and equations which govern and describe the various facets of this project. Some steps of the equation derivations have been omitted since derivations are provided in sufficient detail in most fluid mechanics references.

2.2.1 LAMINAR FLOW EQUATIONS

2.2.1.1 Conservation of Mass and Momentum:

If an Eulerian description is applied to a laminar flow field and constant density is assumed, the following continuity (conservation of mass) equation results.

$$\frac{\partial}{\partial x_i}(U_i) = 0 \quad (1)$$

The conservation of momentum equations are given by Eq(2), which is written in conservative form.

$$\frac{\partial U_i}{\partial t} + \frac{\partial}{\partial X_j}(U_i U_j) = -\frac{1}{\rho} \frac{\partial P}{\partial X_i} + g_i + \nu \nabla^2 U_i \quad (2)$$

Where $U_i, i=1,2,3$,three components of the velocity vector.

2.2.1.2 Energy Equation:

If the conservation of energy is considered for a fluid engaged in laminar flow, the following equation represents the transport of heat within the flow field.

$$\frac{\partial T}{\partial t} + \frac{\partial}{\partial X_i}(U_i T) = \alpha (\nabla^2 T) \quad (3)$$

2.2.2 TURBULENT FLOW EQUATIONS

2.2.2.1 Mean-Value Approach to Turbulence

Turbulent flow has two primary characteristics, random and chaotic fluctuations in the fluid's velocity, and intense mixing on the macroscopic level. These fluctuations and mixing create a fluid motion so complex that the exact details of the motion are undeterminable by a direct analytic approach. Therefore, solutions must be obtained using either a statistical or mean-value approach. Although the parameters associated

with turbulent flow exhibit random fluctuations, these properties may be expressed instantaneously as the sum of the mean value and an instantaneous fluctuation (a'). Thus, for any property (A) in a flow field, its instantaneous value may be expressed as

$$A = \bar{A} + a' \quad (4)$$

Where the mean value is defined by the following equation.

$$\bar{A} = \frac{1}{\Delta t} \int_{t_1}^{t_2} A dt \quad (5)$$

Where

$$\Delta t = t_2 - t_1$$

The time increment (Δt) of Eq(5) is considered large in comparison to the period of the fluctuations. Because Eq(5) is true for any lower limit of the integration, the following equation is true for most practical situations.

$$\frac{\partial \bar{A}}{\partial t} = 0 \quad (6)$$

Applying the mean-value theory of Eq(4) to the properties within a flow field, the following equations are obtained for the velocity components.

$$\begin{aligned} U &= \bar{U} + u' \\ V &= \bar{V} + v' \\ W &= \bar{W} + w' \end{aligned} \quad (7)$$

The density and pressure may also be represented in the same way. However, any changes in density are assumed to be the result of temperature changes within the flow field.

2.2.2.2 Turbulent Flow Equations – Continuity

If the velocity expressions of Eq(7) are substituted into the continuity equation of Eq(1), the following equation results after a time average is taken.

$$\frac{\partial \overline{U}_i}{\partial X_i} = 0 \quad (8)$$

Subtracting Eq(8) from Eq(1),

$$\frac{\partial U_i'}{\partial X_i} = 0 \quad (9)$$

Thus, both the mean and fluctuating velocity components must individually satisfy the continuity equation. It is important to note that these equations are based strongly on the assumption that no turbulent density fluctuations exist. For most practical flow situations, it is generally sufficient to ignore Eq(9) and focus only on the continuity equation of the mean flow [Hinze, 1987].

2.2.2.3 Turbulent Flow Equations - Momentum

If the velocity expressions of Eq(7) are substituted into the momentum equation, Eq(2), and a time average is taken, the following equation will result.

$$\frac{\partial \overline{U}_i}{\partial t} + \frac{\partial}{\partial X_j} (\overline{U_i U_j}) + \frac{\partial}{\partial X_j} (\overline{U_i' U_j'}) = -\frac{\partial}{\partial X_i} \left(\frac{P}{\rho} \right) + g_i + \nu \nabla^2 \overline{U}_i \quad (10)$$

Eq(10) may be manipulated slightly to distinguish the right-hand side of the equation as containing both viscous and turbulent (Reynolds) stresses as shown by the following equation.

$$\rho \frac{\partial \overline{U}_i}{\partial t} + \rho \frac{\partial}{\partial X_j} (\overline{U_i U_j}) = -\frac{\partial P}{\partial X_i} + \rho g_i + \frac{\partial}{\partial X_j} \left(\mu \frac{\partial \overline{U}_i}{\partial X_j} \right) + \frac{\partial}{\partial X_j} (-\rho \overline{u_i' u_j'}) \quad (11)$$

The fact that these Reynolds stresses consist of correlations of velocity fluctuations render the stresses impossible to solve. This incapacity to predict the correlations is known as the "Closure Problem." As a result, exact solutions are not possible.

2.2.3 Turbulence Modeling Theory:

Turbulence models were developed to meet the need for computational results . Turbulence models consist of a set of several equations which, when solved in conjunction with the proper forms of the momentum and continuity equations, approximate the behavior of the Reynolds stresses. Numerous models have been introduced through the years, with varying degrees of success. The success of a model is determined by the following three criteria.

- *Accuracy* - The model must be capable of providing solutions which are within tolerable bounds of accepted experimental results and the basic governing equations of fluid dynamics.
- *Generality* - The model must be capable of being implemented into a wide variety of flow conditions and geometry without requiring significant changes.
- *Easiness* - Although computational capabilities have significantly increased, Implemented overly-complex models may increase the required computational time beyond the limits of feasibility.

Turbulence models are divided into the following classes, based on the number of additional partial-differential equations which must be solved.

- *Zero Equation Model* - The turbulence is described through the use of algebraic equations. Thus, the only partial differential equations requiring solution are the mean flow continuity and momentum equations.
- *One Equation Model* - A partial-differential equation for the turbulent velocity scale is solved in -addition to the mean flow partial-differential equations.
- *Two Equation Model* - Two partial-differential equations for the turbulent velocity scales are solved in addition to the mean flow equations.

Although there are numerous models which may be employed, this study makes use of a two-equation model. Rodi [1980] have given descriptions of the other models.

$$\frac{\partial}{\partial x_j} (\rho \bar{U}_i \bar{U}_j) = -\frac{\partial P}{\partial x_i} + \frac{\partial}{\partial x_j} \left(\mu \frac{\partial \bar{U}_i}{\partial x_j} - \rho \overline{u'_i u'_j} \right) + g_i (\rho - \rho_0)$$

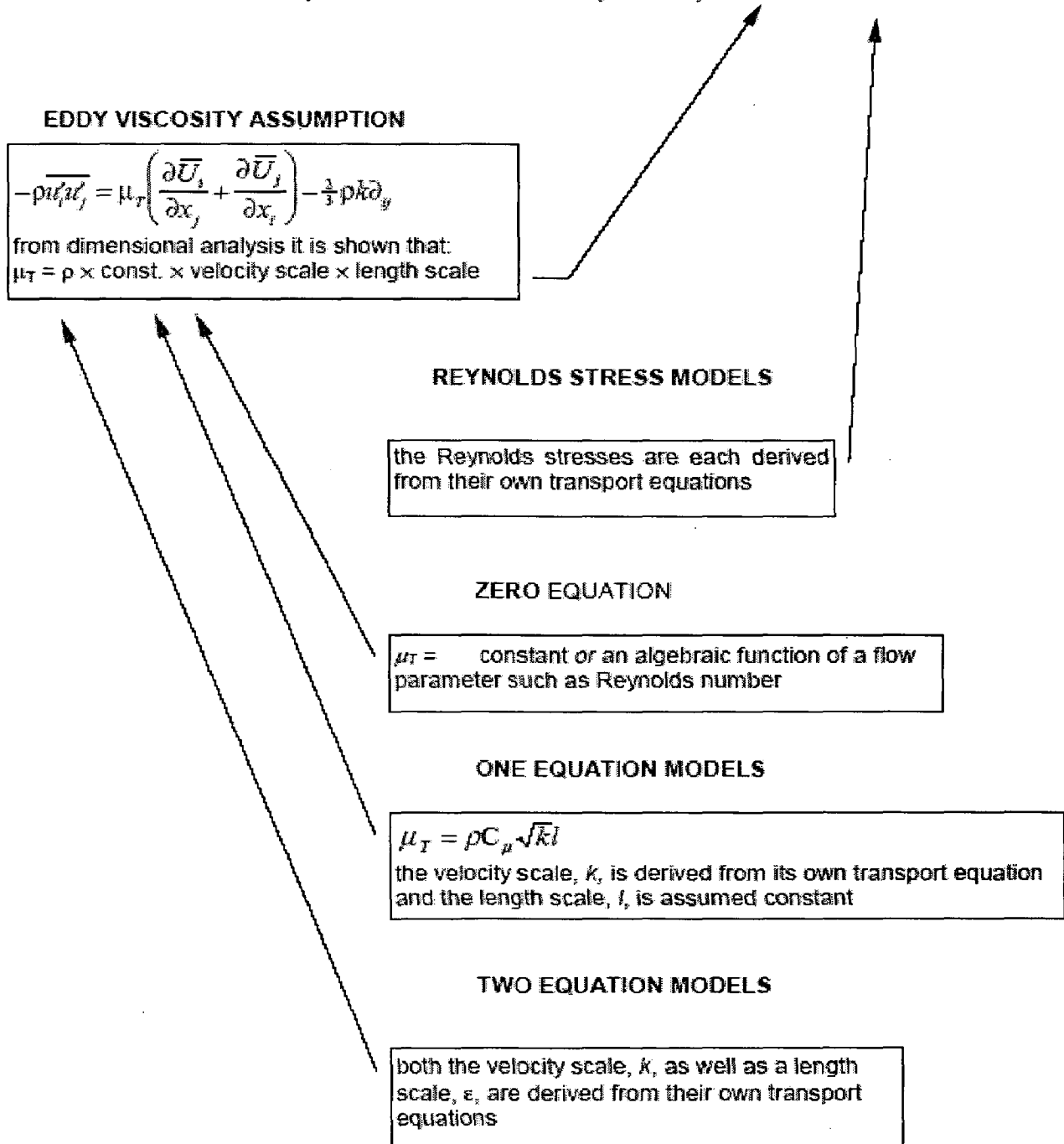


Fig 2.1 Tree of turbulence modeling

2.2.3.1 k- ε Turbulence Model:

To numerically simulate the turbulent flow, this study uses the k- ε turbulence model. It is a two-equation model which couples differential equations for the turbulent kinetic energy (k) and the turbulence dissipation rate (ε). The mathematics of the model begin by defining the turbulent kinetic energy as

$$k = \frac{1}{2} \overline{u_i u_i} \quad (12)$$

The Reynolds stresses of Eq(11) are then modeled by the product of a new term, the turbulent viscosity (ν_t), and the mean velocity gradient as shown by

$$\overline{u_i u_j} = \nu_t \left(\frac{\partial U_i}{\partial X_j} + \frac{\partial U_j}{\partial X_i} - \frac{2}{3} k \delta_{ij} \right) \quad (13)$$

Where $\delta_{ij} = 1$ for $i = j$
 $= 0$ for $i \neq j$

If this new expression for the Reynolds stresses is substituted into the momentum equation, the following new equation may be used as the conservation of momentum equation for turbulent flow. Note that the viscous stress is assumed negligible and that the equation is now coupled with the turbulent kinetic energy.

$$\frac{\partial U_i}{\partial t} + \frac{\partial}{\partial X_j} (U_i U_j) = \frac{\partial}{\partial X_j} \left(\frac{P}{\rho} \right) + g_i + \frac{\partial}{\partial X_j} \left(\nu_t \left(\frac{\partial U_i}{\partial X_j} + \frac{\partial U_j}{\partial X_i} \right) - \frac{2}{3} k \delta_{ij} \right) \quad (14)$$

Above equation uses the mean velocity values. This turbulent viscosity term (ν_t) is not a property of the fluid in the same way as the Newtonian viscosity. Rather, it is dependent upon the structure of the turbulence in the flow and may differ at various points throughout the flow. The turbulent viscosity may be determined empirically from Eq(15), although it is only one of several possible choices for the turbulent viscosity equation.

$$\nu_t = C_\mu \frac{k^2}{\varepsilon} \quad (15)$$

Where $C_\mu = 0.09$

The resulting transport equations for the turbulent kinetic energy and its rate of dissipation are shown in the following equations. Again, it must be emphasized that only a very brief summary of this model is being presented. Further detail may be found in Rodi [1980] or Hinze [1987], as these references were used extensively in the development of this summary.

$$R_\nu = \frac{U_o L_o}{\nu} \quad (16)$$

$$\frac{\partial \varepsilon}{\partial t} + \frac{\partial}{\partial X_j} (U_j \varepsilon) = \frac{\partial}{\partial X_j} \left(\frac{\nu_t \partial \varepsilon}{\sigma_\varepsilon \partial X_j} \right) + \frac{C_1 \nu_t \varepsilon}{k} \frac{\partial U_i}{\partial X_j} \left(\frac{\partial U_i}{\partial X_j} + \frac{\partial U_j}{\partial X_i} \right) - C_2 \frac{\varepsilon^2}{k} \quad (17)$$

It is very important to realize that intermediate steps in the derivation of Eq(16) and Eq(17) result in the presence of higher order correlations. The unsolvable nature of these correlations is alleviated by modeling the correlations in the equations. The recommended values of the empirical constants and functions are given in Table 2.1. These values represent what is considered the "standard" k- ε model.

Table 2.1 CONSTANTS FOR THE "STANDARD" k- ε MODEL
[Launder, 1974]

C_μ	C_1	C_2	σ_k	σ_ε
0.09	1.44	1.92	1.0	1.3

Justification for k- ε Use:

While detailed derivations of other turbulence models are not included, the justification for the use of the k- ε model should be addressed. With all of the potential turbulence models available, it is certainly valid to question the preference of one model over the others. As discussed later in the literature review, all the researchers modeling room air flow have used the k- ε model.

Some of the researchers commented on the reason for the model's use, while others implied its use due to popularity. This "popularity" argument contains a reasonable

amount of validity. Using the same model as others should allow a better comparison of numerical results, as it eliminates a variable in the experimental process.

The model's popularity also reduces the implementation difficulty since there are several references available discussing the numerical aspects of modeling turbulence through the use of the $k-\varepsilon$ equations. Because the $k-\varepsilon$ model is a two-equation model, improved accuracy is obtained in comparison to less-complicated models. Researchers investigating some of the primary two-equation models have discovered that only the $k-\varepsilon$ model yields experimentally substantiated results for regions far from solid boundaries or walls [Launder, 1974;Launder, et al., 1972]. For the other models to match the results, it was found necessary to replace some of the constants with empirical functions which added to the complexity of the models.

2.2.3.2 LOW-REYNOLDS NUMBER MODEL:

When discussing turbulent flow, it is convenient to mention an additional parameter, the Turbulent Reynolds Number (R_T) is used in turbulent flows.

$$R_T = \frac{k^2}{\varepsilon \nu} \quad (19)$$

Due to the nature of room air flow, there will always be regions (particularly near the walls) in which this number is quite small. In these regions, the viscous effects become significantly greater than any turbulent effects. Because the standard form of the $k-\varepsilon$ model is valid only for high Reynolds number turbulent flows, difficulty arises. There are two ways in which the fully turbulent $k-\varepsilon$ model may be used for low-Reynolds number flow. These methods are known as wall functions and low-Reynolds models.

The wall functions, when used in conjunction with the standard $k-\varepsilon$ equations, are intended to reproduce the logarithmic velocity profile of a turbulent boundary layer near the wall. No changes are made to the $k-\varepsilon$ equations. Instead, the velocity profile is created through the use of complex expressions imposed as boundary conditions at the walls. A detailed derivation and explanation is not included, equations Eq(19) -

Eq(22) represent wall functions introduced by Launder and Spalding [1974]. It is important to note in the following equations that values with the "wall" subscript (w) denote values at the wall, while values of, U_t , k and ε are values at the first node adjacent to the wall.

$$\frac{U_t}{\tau_w / \rho} (C_\mu^{1/2} k)^{1/2} = \frac{1}{k} \ln \left(\frac{E y_n (C_\mu^{1/2} k)^{1/2}}{\nu} \right) \quad (19)$$

$$\left(\frac{\nu_t}{\sigma_k} \frac{\partial k}{\partial y_n} \right)_{wall} = 0 \quad (20)$$

$$\varepsilon^* = \frac{(C_\mu^{1/2} k)^{3/2}}{k y_n} \ln \left(\frac{E y_n (C_\mu^{1/2} k)^{1/2}}{\nu} \right) \quad (21)$$

$$\varepsilon = \frac{(C_\mu^{1/2} k)^{3/2}}{k y_n} \quad (22)$$

Where k = von Karman's constant (0.4).

τ_w = shear stress at the wall.

E = function determined by wall roughness (9.0 for a smooth wall).

ε^* = value of ε used in the k -equation.

ε = value of ε used in the ε -equation

Wall functions have the significant benefits of reducing computational needs as well as allowing the addition of other empirical functions necessary for special boundary conditions. The primary concern with this method is that the high-Reynolds k - ε model with the logarithmic wall functions may not be suitable for use both near the wall and far away from it [Chen, 1990]. In addition, the traditional wall functions may not be appropriate for complex three-dimensional flow. The second method for describing low-Reynolds number flow involves modifying the standard k - ε equations, making them valid throughout the full range of flow regions (laminar,

buffer, and fully turbulent). Changes are made through the addition of the empirical functions F_μ , F_1 , F_2 , and E , as shown in the following low-Reynolds equations.

$$\frac{\partial k}{\partial t} + \frac{\partial}{\partial X_j}(U_j k) = \frac{\partial}{\partial X_j} \left(\frac{\nu_t}{\sigma_k} \frac{\partial k}{\partial X_j} \right) + \nu_t \frac{\partial U_i}{\partial X_j} \left(\frac{\partial U_i}{\partial X_j} + \frac{\partial U_j}{\partial X_i} \right) - \varepsilon \quad (23)$$

$$\frac{\partial \varepsilon}{\partial t} + \frac{\partial}{\partial X_j}(U_j \varepsilon) = \frac{\partial}{\partial X_j} \left(\frac{\nu_t}{\sigma_\varepsilon} \frac{\partial \varepsilon}{\partial X_j} \right) + \frac{C_1 F_1 \nu_t \varepsilon}{k} \frac{\partial U_i}{\partial X_j} \left(\frac{\partial U_i}{\partial X_j} + \frac{\partial U_j}{\partial X_i} \right) - C_2 F_2 \frac{\varepsilon^2}{k} + E \quad (24)$$

$$\nu_t = C_\mu F_\mu \frac{k^2}{\varepsilon} \quad (25)$$

$$R_\tau = \frac{k^2}{\nu \varepsilon} \quad (26)$$

$$R_y = \frac{\sqrt{k}}{\nu} y_n \quad (27)$$

Where y_n = distance normal to the wall (m)

The following table 2.2 contains the various empirical constants for three of the more popular low-Reynolds number $k-\varepsilon$ models. For comparison, values are also given for the standard, high-Reynolds number model.

Table 2.2 **LOW-REYNOLDS $k-\varepsilon$ CONSTANTS**
[Patel, 1984]

Model	C_μ	C_1	C_2	σ_k	σ_ε
Standard	0.09	1.44	1.92	1.0	1.3
Launder-Sharma	0.09	1.44	1.92	1.0	1.3
Chien	0.09	1.35	1.8	1.0	1.3
Lam-Bremhorst	0.09	1.44	1.92	1.0	1.3

The following table 2.3 contains the values and expressions for the empirical functions which have been added to the original $k-\varepsilon$ equations to model low-Reynolds number flow.

Table 2.3

LOW REYNOLDS K- ε FUNCTIONS [Patel,1984]

Model	F_μ	F_1	F_2	E
Standard	1	1	1	0
Launder-sharma	$\exp\left(\frac{-3.4}{\left(1+\frac{R_T}{50}\right)^2}\right)$	1	$1-0.3\exp(-R_T^2)$	$2\nu\nu_t\left(\frac{\partial^2 u}{\partial y_n^2}\right)^2$
chien	$1-\exp(-0.0115y^+)$	1	$1-0.22\exp(-(R_T/6)^2)$	$\frac{-2\nu\varepsilon}{y^2}\exp(-0.5y^+)$
Lam-Bremhorst	$\left[1-\exp(-0.0165R_y)\right]^2 * \left(1+\frac{20.5}{R_T}\right)$	$1+\left(\frac{0.05}{F_\mu}\right)^3$	$]1-\exp(-R_T^2)$	0

The "standard" k- ε model for fully turbulent flow is a special case of the low-Reynolds equations of Eq(23) and Eq(24). Therefore, a solution algorithm could easily employ the wall function or low-Reynolds algorithms by simply using the corresponding values of, F_μ , F_1 , and F_2 .

2.2.3.3 LARGE EDDY SIMULATION:

The velocity field with in a room is described by the equations of continuity and momentum. Those equations are shown in eq (1) and eq(2).

In large eddy simulation, any physical quantity f is decomposed in to two parts:

$$f = \bar{f} + f'' \quad (28)$$

Here, \bar{f} is the resolvable-scale component and f'' is the subgrid-scale component.

\bar{f} is defined with a filter function $G(X,Y)$ as follows:

$$\bar{f}(X) = \iiint_{-\infty}^{\infty} G(X,Y) f(Y) dY \quad (29)$$

Here, a top-hat filter function is used as $G(X,Y)$,

$$G(X,Y)= \begin{cases} \prod_{i=1}^3 \frac{1}{\Delta_i} & |x_i - y_i| \leq \frac{1}{2} \Delta_i \\ 0 & |x_i - y_i| > \frac{1}{2} \Delta_i \end{cases} \quad (30)$$

Where Δ_i is the computational grid size in the x_i direction, X, Y is a position vector.

Imposing function (29) on eq 1,2 filtered equations are given as follows:

$$\frac{\partial \bar{U}_i}{\partial x_i} = 0 \quad (31)$$

$$\frac{\partial \bar{U}_i}{\partial t} + \frac{\partial \bar{U}_i \bar{U}_j}{\partial x_j} = -\frac{1}{\rho} \frac{\partial \bar{p}}{\partial x_i} + \frac{\partial}{\partial x_j} \left[-\overline{U_i'' U_j''} - \overline{U_i'' \bar{U}_j} - \overline{\bar{U}_i U_j''} - (\overline{\bar{U}_i \bar{U}_j} - \bar{U}_i \bar{U}_j) + \nu \frac{\partial \bar{U}_i}{\partial x_j} \right] \quad (32)$$

In this study, Reynolds averaging assumption is applied:

$$\overline{\bar{U}_i \bar{U}_j} - \bar{U}_i \bar{U}_j + \overline{U_i'' \bar{U}_j} + \overline{\bar{U}_i U_j''} = 0 \quad (33)$$

Then we get

$$\frac{\partial \bar{U}_i}{\partial t} + \frac{\partial \bar{U}_i \bar{U}_j}{\partial x_j} = \frac{\partial p^*}{\partial x_i} + \frac{\partial}{\partial x_j} \left[-\left(\overline{U_i'' U_j''} - \frac{1}{3} \overline{U_i'' U_j''} \delta_{ij} \right) + \nu \frac{\partial \bar{U}_i}{\partial x_j} \right] \quad (34)$$

$$\text{Where } p^* = \frac{p}{\rho} + \frac{1}{3} \overline{U_i'' U_i''}$$

Here, Reynolds number is assumed to be very large so that the viscous term can be neglected. The viscous sublayer at the wall is not treated explicitly.

In equation (34), \bar{U}_i and p^* are variables whose values are computed at mesh points of the computational field.

2.3 OTHER MODELS

This section presents brief descriptions of the published literature and recorded experimental results in the field of room air flow modeling and prediction. The list is not exhaustive, the review should sufficiently represent the advances, findings, and contributions which are of particular relevance to this project.

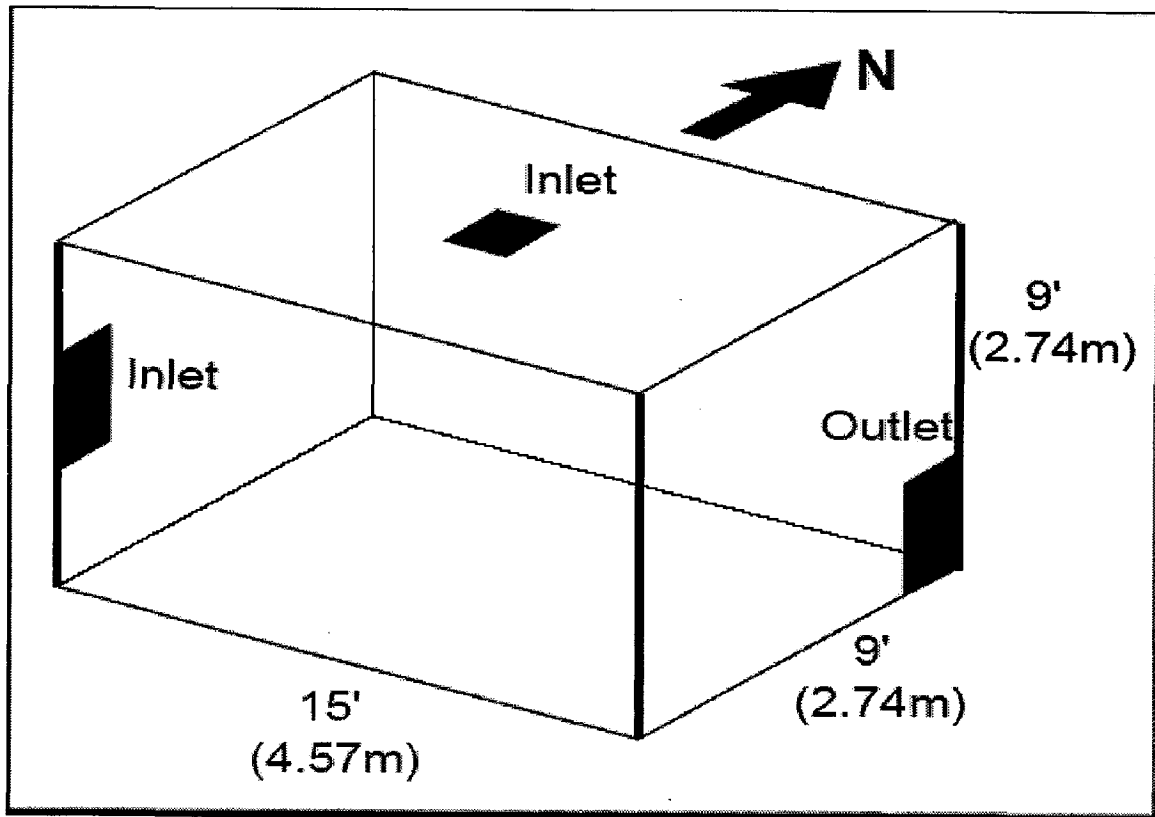


Fig 2.2 Experimental facility
[Spitler 1990]

In all of the room configurations, one ventilation outlet located on the east wall was used (see Figure 2.1). The dimensions of the inlets and outlets are shown in Table 2.5. With the presentation of Table 2.5, it is important to note how inlet dimensions are generally used in room air flow studies to define non-dimensional parameters and distances. Throughout this report, dimensional distances are presented. In addition, results will be presented by defining distances with respect to the inlet width. Thus, $y/W=2$ would correspond to a distance equal to twice the inlet width.

Table 2.5**INLET AND OUTLET DIMENSIONS**
[Spitler, 1991]

Location	Width (m)	Length (m)	Width (m)	Length (m)
Side Wall Inlet	15.75	35.58	0.40	0.90
Ceiling Inlet	15.75	15.75	0.40	0.40
East Outlet	15.75	35.58	0.40	0.90

The ventilation system was capable of providing between 2 and 100 ACH ("air changes per hour") of ventilation. This corresponds to volumetric flow rates of 40.5 -2025 cfm (0.019 - 0.945 m³/s). A total of 44 separate experimental tests were performed, as described in Table 2.6. The use of the 53 controllable panels is of particular interest to the modeling aspect of this study. By controlling the temperature of the walls, the convective heat fluxes were measured and film coefficients for all surfaces were calculated. This data allows the imposition of temperature boundary conditions which are consistent with experimental data.

Table 2.6**EXPERIMENTAL TESTS**
[Spitler, 1991]

Configuration	Inlet Temperature (°C)	Ventilation Rate (ACH)
1	16, 21, 26	15, 30, 50, 70, 100
2	16, 21, 26	15, 30, 50, 70, 100
3	21	15, 30, 50, 70
4	21	15, 30, 70
5	21	15, 30, 70
6	21	30, 70
7	21	30, 70

Patel

An extensive review of the $k-\epsilon$ model for low Reynolds number flow was compiled by Patel [Patel, 1985]. In addition to the nature and derivation of the model, Patel also detailed the following seven variations or extensions of the model:

1. Launder-Sharma
2. Hassid-Poreh
3. Hoffman
4. Dutoya-Michard
5. Chien
6. Reynolds
7. Lam-Bremhorst

In an attempt to compare the models, each model was implemented with the addition of the following equations to numerically predict flow in a two-dimensional boundary layer.

$$\frac{\partial U}{\partial X} + \frac{\partial V}{\partial Y} = 0 \quad (35)$$

$$U \frac{\partial U}{\partial X} + V \frac{\partial U}{\partial Y} = -\frac{1}{\rho} \frac{\partial P}{\partial X} + \frac{\partial}{\partial Y} \left(\nu \frac{\partial U}{\partial Y} - \overline{UV} \right) \quad (36)$$

The proposed models of Hassid-Poreh, Hoffman, Dutoya-Michard, and Reynolds failed to reproduce the simple case of this flat-plate boundary layer. Comparable results to experimental data were achieved through the use of the Launder-Sharma, Chien, and Lam-Bremhorst models. Despite these successful results, a refinement to the models was determined necessary if near-wall and low Reynolds number flows were to be calculated.

Patel offered the following suggestions:

1. Select a damping function for the shear stress which is in agreement with experimental evidence.
2. Choose the low Reynolds number functions in the dissipation rate equation with a mathematically consistent near-wall behavior.
3. "Fine tune" the functions to ensure that well-published features of wall bounded shear flows over a range of pressure gradients would be produced.
4. Distinct improvement of the predictions for adverse pressure gradient flows would require additional modifications to the high Reynolds number models.

Lam and Bremhorst

Since the emergence of the $k-\varepsilon$ turbulence model, numerous researchers have introduced modifications to the basic models, particularly in an attempt to accurately predict low-Reynolds number turbulent flow. Perhaps one of the more significant modifications was introduced by Lam and Bremhorst [Lam & Bremhorst, 1981]. As with the previous models, the turbulent energy and its dissipation rate were modeled using Eq(23) and (24). The constants being used were the same as the original model: $\sigma_K=1.0$, $\sigma_\varepsilon=1.3$, $C_\mu=0.09$, $C_1=1.44$, and $C_2=1.92$.

The primary difference exists in the functions F_μ , F_1 , and F_2 in the low-Reynolds equations of Eq(23) and Eq(24). Previously, the values of these functions were assumed to be equal, or very close to unity. The research of Lam and Bremhorst found these assumptions to be invalid within a laminar or viscous sub layer. A new equation for F_μ was found to be

$$F_\mu = (1 - \exp(-A_\mu R_y))^2 \left(1 + \frac{A_t}{R_t} \right) \quad (37)$$

Where $A_\mu = 0.0165$ $A_t = 20.5$

This new equation is directly influenced by the presence of a wall, as F_μ will approach unity at large distances from a wall for increasingly high levels of turbulence

The proposed equation for F_1 was

$$F_1 = 1 + \left(\frac{0.05}{F_\mu} \right)^3 \quad (38)$$

Investigation showed that if F_1 was equal to unity, as previously assumed, additional terms would be required in the $k-\varepsilon$ equations to yield reasonable results. In an effort to produce an equation which approaches zero as R_T approaches zero, the following equation for F_2 was introduced.

$$F_2 = 1 - \exp(-R_f^{-2}) \quad (39)$$

This new low-Reynolds form of the k-ε model was tested by applying the technique to the case of fully developed turbulent pipe flow. Strong agreement was found with the experimental data. The principle advantage, as emphasized by the researchers, is that the presence of a wall function formula is not required.

Chen

As discussed earlier, one of the particular difficulties with modeling room air flow is that the k-ε model, although suitable for fully turbulent flow, requires the use of empirical functions near the wall. Chen explored the wall function problem as he attempted to accurately prediction low-Reynolds, turbulent, buoyant flow [Chen, 1990]. Chen used the Lam-Bremhorst version of the k-ε model [Lam & Bremhorst, 1981] to predict natural convection flow within cavities. This version of the model was chosen based on recommendations by previous researchers [Patel, 1985] and its relative ease of implementation into a computer algorithm. It was assumed that any temperature gradients within the cavity were small, therefore the use of Boussinesq approximation for buoyancy was performed through the addition of the following term in the momentum equations.

$$\beta g_i (T - T_o) \quad (40)$$

The effects of buoyancy in the turbulence equations were approximated using the following terms in the k-ε equations.

$$S_k = \frac{\beta v_i}{\sigma_h} \frac{\partial}{\partial X_i} (T - T_o) g_i \quad (41)$$

$$S_\epsilon = \frac{1.44 \epsilon S_k}{k} \quad (42)$$

These source terms would then be included in the right-hand side of Eq(23) and Eq(24)

The first of the two simulations was performed on a small-scale, water-filled cavity. The second simulation was made on a full-scale, air filled cavity. The resulting velocity profiles were in good agreement with the measured values. However, the high-Reynolds number $k-\varepsilon$ model with wall functions produced results which differed by as much as 61% from the experimental results.

Awbi

Perhaps the most significant application of CFD analysis in room air flow may be in the area of ventilation. Studies have shown that the thermal condition within a room is dependent on the turbulence intensity of the air motion and frequency of flow fluctuations, in addition to the air velocity and temperature distributions. Awbi presented numerical studies of various ventilation configurations through the use of CFD [Awbi, 1989].

Using the standard $k-\varepsilon$ model, coupled with logarithmic wall functions, simulations were performed on the ventilation of both two and three-dimensional enclosures. Other simulations involved creating a fixed or constant load within the room to better investigate the effects of buoyancy. The numerical solutions produced reasonably good predictions of the velocity vectors within the room when compared to experimental results. Awbi carefully noted, though, that considerably more studies are necessary if CFD techniques are to be used as design tools with any degree of confidence.

Murakami, et al.

Murakami, et al. from the University of Tokyo, have contributed greatly to the study of numerically modeling room air flow. Each study has emphasized different facets of the overall problem, thus providing a better insight concerning the potential for CFD in ventilation design and analysis.

The first investigations were performed with the intention of verifying the validity of a three-dimensional numerical simulation for turbulence [Murakami, et al., 1987]. Simulations were performed and compared to experimental rooms with a 1:6 scale. The experimental rooms were scaled so that the Reynolds number would be identical to a full scale room based on the following equation.

$$R_e = \frac{U_o L_o}{\nu} \quad (43)$$

Where U_o = inlet velocity (m/sec)

L_o = width of supply outlet (m)

The flow domain was covered with a rectangular mesh. Later investigations employed the use of boundary-fitted curvilinear coordinate systems [Murakami, et al., 1989a]. The air temperature was assumed to be completely uniform. Thus, buoyant effects were completely ignored. The high-Reynolds $k-\varepsilon$ equations (Eq(16) and Eq(17)) were solved in conjunction with the momentum equation of Eq(14). The standard values for the equation constants were used and wall functions were used to simulate viscous effects near the wall.

The numerical simulations were reported to correspond "fairly good" with the experimental results from the scaled room. Later investigations focused on the diffusion of particles within a ventilated room, with particular emphasis on the design and analysis of clean rooms [Murakami, et al., 1989b, 1990]. The same sets of equations and wall functions were used to analyze other scaled room configurations. Scaling the room based on the inlet velocity and inlet width is questionable when investigating turbulent room air flow. Scaling in this way does not insure identical turbulent Reynolds numbers. In addition, the development of turbulent jets is based on other parameters which are completely independent of the Reynolds number at the inlet.

The flow modeling is focus on stationary characteristics with a view to assess indoor air quality and thermal comfort. Analysis of the energy use of a room or a building however requires information on the transient characteristics of the indoor climate.

A flow field can be described by the conservation of mass, momentum and energy. Given the boundary conditions, the resulting flow pattern is determined by solving the combined Navier-Stokes and energy or any other scalar equations.

3.1 MATHEMATICAL MODEL:

3.1.1 CONTINUITY EQUATION:

$$\frac{\partial}{\partial x_1}(u_1) = 0 \tag{44}$$

$$\frac{\partial}{\partial x_2}(u_2) = 0 \tag{45}$$

$$\frac{\partial}{\partial x_3}(u_3) = 0 \tag{46}$$

3.1.2 MOMENTUM BALANCE:

$$\frac{\partial}{\partial t}(u_1) + \frac{\partial}{\partial x_1}(u_1 u_1) = -\frac{\partial}{\partial x_1}\left(\frac{p}{\rho} + \frac{2}{3}k\right) + \frac{\partial}{\partial x_1}\left[\mathcal{G}_1\left(\frac{\partial}{\partial x_1}(u_1) + \frac{\partial}{\partial x_1}(u_1)\right)\right] \tag{47}$$

$$\frac{\partial}{\partial t}(u_1) + \frac{\partial}{\partial x_2}(u_1 u_2) = -\frac{\partial}{\partial x_1}\left(\frac{p}{\rho} + \frac{2}{3}k\right) + \frac{\partial}{\partial x_2}\left[\mathcal{G}_1\left(\frac{\partial}{\partial x_2}(u_1) + \frac{\partial}{\partial x_1}(u_2)\right)\right] \tag{48}$$

$$\frac{\partial}{\partial t}(u_1) + \frac{\partial}{\partial x_3}(u_1 u_3) = -\frac{\partial}{\partial x_1}\left(\frac{p}{\rho} + \frac{2}{3}k\right) + \frac{\partial}{\partial x_3}\left[\mathcal{G}_1\left(\frac{\partial}{\partial x_3}(u_1) + \frac{\partial}{\partial x_1}(u_3)\right)\right] \tag{49}$$

$$\frac{\partial}{\partial t}(u_2) + \frac{\partial}{\partial x_1}(u_2 u_1) = -\frac{\partial}{\partial x_2}\left(\frac{p}{\rho} + \frac{2}{3}k\right) + \frac{\partial}{\partial x_1}\left[\mathcal{G}_t\left(\frac{\partial}{\partial x_1}(u_2) + \frac{\partial}{\partial x_2}(u_1)\right)\right] \quad (50)$$

$$\frac{\partial}{\partial t}(u_2) + \frac{\partial}{\partial x_2}(u_2 u_2) = -\frac{\partial}{\partial x_2}\left(\frac{p}{\rho} + \frac{2}{3}k\right) + \frac{\partial}{\partial x_2}\left[\mathcal{G}_t\left(\frac{\partial}{\partial x_2}(u_2) + \frac{\partial}{\partial x_2}(u_2)\right)\right] \quad (51)$$

$$\frac{\partial}{\partial t}(u_2) + \frac{\partial}{\partial x_3}(u_2 u_3) = -\frac{\partial}{\partial x_2}\left(\frac{p}{\rho} + \frac{2}{3}k\right) + \frac{\partial}{\partial x_3}\left[\mathcal{G}_t\left(\frac{\partial}{\partial x_3}(u_2) + \frac{\partial}{\partial x_2}(u_3)\right)\right] \quad (52)$$

$$\frac{\partial}{\partial t}(u_3) + \frac{\partial}{\partial x_1}(u_3 u_1) = -\frac{\partial}{\partial x_3}\left(\frac{p}{\rho} + \frac{2}{3}k\right) + \frac{\partial}{\partial x_1}\left[\mathcal{G}_t\left(\frac{\partial}{\partial x_1}(u_3) + \frac{\partial}{\partial x_3}(u_1)\right)\right] \quad (53)$$

$$\frac{\partial}{\partial t}(u_3) + \frac{\partial}{\partial x_2}(u_3 u_2) = -\frac{\partial}{\partial x_3}\left(\frac{p}{\rho} + \frac{2}{3}k\right) + \frac{\partial}{\partial x_2}\left[\mathcal{G}_t\left(\frac{\partial}{\partial x_2}(u_3) + \frac{\partial}{\partial x_3}(u_2)\right)\right] \quad (54)$$

$$\frac{\partial}{\partial t}(u_3) + \frac{\partial}{\partial x_3}(u_3 u_3) = -\frac{\partial}{\partial x_3}\left(\frac{p}{\rho} + \frac{2}{3}k\right) + \frac{\partial}{\partial x_3}\left[\mathcal{G}_t\left(\frac{\partial}{\partial x_3}(u_3) + \frac{\partial}{\partial x_3}(u_3)\right)\right] \quad (55)$$

3.1.3 TRANSPORT EQUATION FOR k :

$$\frac{\partial}{\partial t}(k) + \frac{\partial}{\partial x_1}(k u_1) = \frac{\partial}{\partial x_1}\left(\frac{\mathcal{G}_t}{\sigma_1} \frac{\partial}{\partial x_1} k\right) + \mathcal{G}_t s - \varepsilon \quad (56)$$

$$\frac{\partial}{\partial t}(k) + \frac{\partial}{\partial x_2}(k u_2) = \frac{\partial}{\partial x_2}\left(\frac{\mathcal{G}_t}{\sigma_1} \frac{\partial}{\partial x_2} k\right) + \mathcal{G}_t s - \varepsilon \quad (57)$$

$$\frac{\partial}{\partial t}(k) + \frac{\partial}{\partial x_3}(k u_3) = \frac{\partial}{\partial x_3}\left(\frac{\mathcal{G}_t}{\sigma_1} \frac{\partial}{\partial x_3} k\right) + \mathcal{G}_t s - \varepsilon \quad (58)$$

3.1.4 TRANSPORT EQUATION FOR ε

$$\frac{\partial}{\partial t}(\varepsilon) + \frac{\partial}{\partial x_1}(\varepsilon u_1) = \frac{\partial}{\partial x_1}\left(\frac{\mathcal{G}_t}{\sigma_2} \frac{\partial}{\partial x_1} \varepsilon\right) + C_1 \frac{\varepsilon}{k} \mathcal{G}_t s - C_2 \frac{\varepsilon^2}{k} \quad (59)$$

$$\frac{\partial}{\partial t}(\varepsilon) + \frac{\partial}{\partial x_2}(\varepsilon u_2) = \frac{\partial}{\partial x_2}\left(\frac{\mathcal{G}_t}{\sigma_2} \frac{\partial}{\partial x_2} \varepsilon\right) + C_1 \frac{\varepsilon}{k} \mathcal{G}_t s - C_2 \frac{\varepsilon^2}{k} \quad (60)$$

$$\frac{\partial}{\partial t}(\varepsilon) + \frac{\partial}{\partial x_3}(\varepsilon u_3) = \frac{\partial}{\partial x_3}\left(\frac{\mathcal{G}_t}{\sigma_2} \frac{\partial}{\partial x_3} \varepsilon\right) + C_1 \frac{\varepsilon}{k} \mathcal{G}_t s - C_2 \frac{\varepsilon^2}{k} \quad (61)$$

$$g_i = k^{0.5} l = C_0 k^2 / \varepsilon$$

$$\sigma_1 = 1.0 \quad C_0 = 0.09$$

$$\sigma_2 = 1.3 \quad C_1 = 1.44$$

$$C_2 = 1.92$$

$$s = \left(\frac{\partial}{\partial x_j} (u_i) + \frac{\partial}{\partial x_i} (u_j) \right) \frac{\partial}{\partial x_j} (u_i)$$

3.2 BOUNDARY CONDITIONS

The equations described in the above section are solved to predict the air velocity and temperature distribution in mechanically ventilated (heated or cooled) rooms. Since the boundary conditions are unique to a particular flow situation, an accurate representation of these conditions is necessary for a reliable solution to be achieved. For the ventilated rooms it is necessary to specify the conditions as inlet, outlet and on the internal surfaces of the room. In general three types of boundary conditions are used.

3.2.1 INLET CONDITION:

Uniform distribution is used over the inlet boundary of the longitudinal velocity, u_0 , temperature, T , kinetic energy of turbulence, k , and the energy dissipation rate, ε . Other quantities such as pressure and the other two velocity components are taken as zero at the inlet.

The kinetic energy of turbulence is calculated using

$$k = (3/2) I^2 u_0^2 \quad (62)$$

Where I^2 is the turbulence intensity of the u -component of velocity at the inlet which is taken as 0.14 in the absence of measured values,

The dissipation rate is obtained from

$$\varepsilon = k^{1.5} / (\lambda H) \quad (63)$$

Where λ is a constant taken as 0.005 and H is the room height or the square root of the cross sectional area of the room.

3.2.2 OUTLET CONDITIONS:

The longitudinal component of velocity u_e is derived from the continuity equation, i.e

$$u_e = u_o \frac{A_o \rho_o}{A_e \rho_e} \quad (64)$$

and the other velocity components and the pressure are assumed to be zero. The exit temperature T_e is obtained from the energy equation for the whole flow field taking into account heat transfer across all boundaries. Boundary conditions for k and ε are not required because an up-wind computational scheme, is used expect that their gradients in the exit plane are zero. Uniform distribution of u_e and T_e is assumed across the exit area.

3.2.3 WALL BOUNDARY:

Close to a wall region laminar viscosity becomes more significant than turbulent viscosity as a result of the damping effect of the wall, i.e $\frac{\partial}{\partial y}(k) = 0$ at the wall. So

the turbulence model equations do not apply to regions close to a solid boundary and instead the wall-function equations due to lauder and spalding are used for the velocity component parallel to the boundary. With in the laminar sublayer region viscous effects pre-dominate and the wall shear stress, τ_w , is described by the usual couette flow expression. At a point outside this region turbulent shear becomes significant and it can be shown that when the generation and dissipation of energy is in balance then $\frac{\tau}{\rho} = C_\mu^{0.5} k$

The boundary temperatures can be specified to represent the actual temperatures of the room surfaces or to represent the temperature of a heat source or a sink of a known capacity. Heat fluxes or sinks can be treated as additional source terms in the energy equation.

Using proper commands of GAMBIT modeling, geometrical model (of physical model) has developed.

The common faces (interfaces) of the volumes were connected. The room dimensions are 6 m width,6 m long ,6 m height. The inlet is given in side face as rectangular shape with width of 1m and height of 2 m. The two outlets are on the opposite side face as circular shape wit radius of 0.5 m at a distance 1.5 m from center on that face. The oulets height from bottom is 4 m.

The obtained model is as shown in the figure 4.1 to 4.3

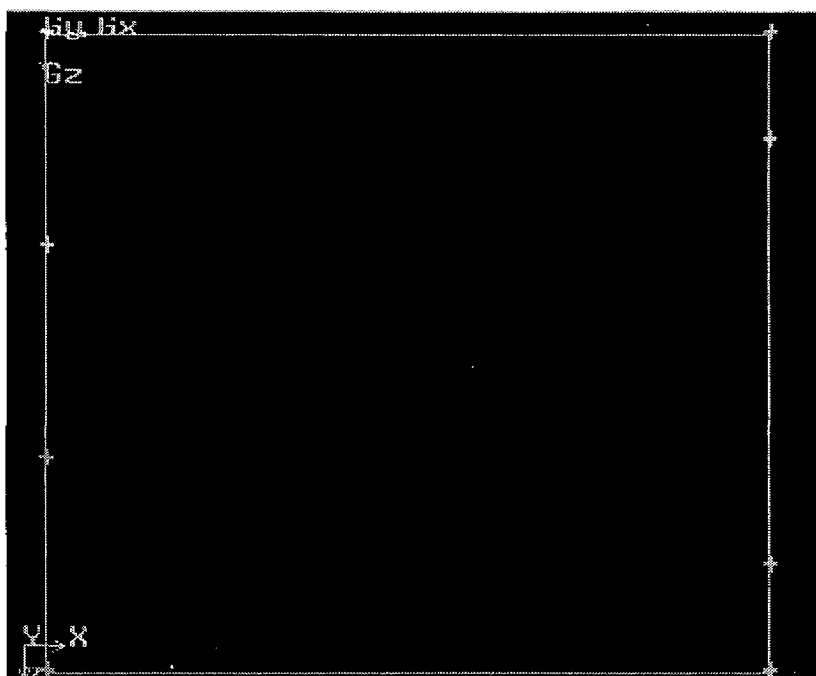


Fig . 4.1 Top view

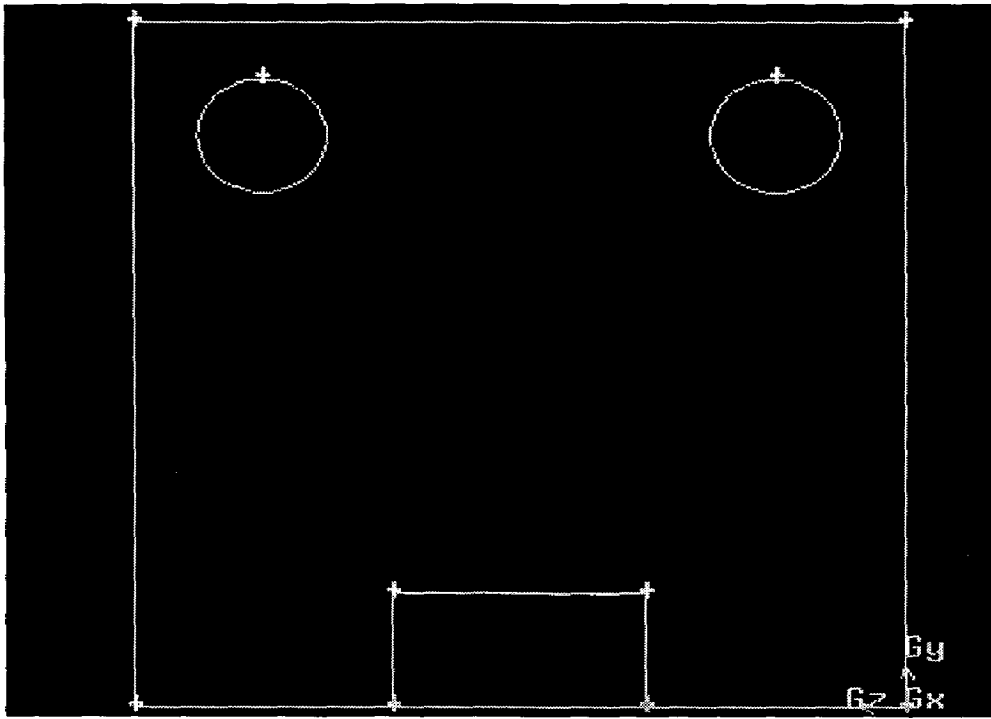


Fig. 4.2 side view

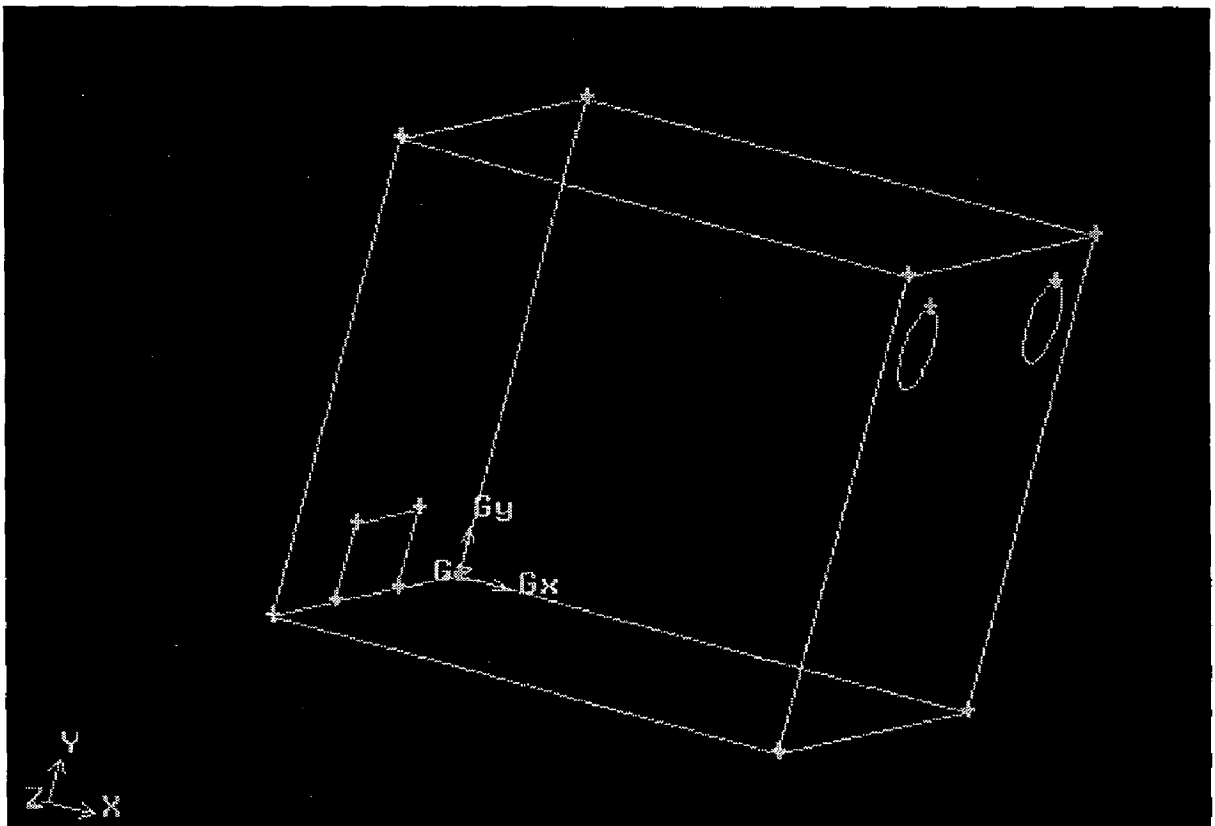


Fig. 4.3 Isometric view

4.2 MESH GENERATION

Meshing Scheme used:

Elements choosen : Hex

The Elements parameter defines the shape of the elements that are used to mesh the volume. Hex specifies that the mesh includes only hexahedral elements.

Type choosen : Cooper

The Type parameter defines the meshing algorithm and therefore, the overall pattern of mesh elements in the volume. Cooper algorithm aweeeps the mesh node patterns of specified source faces through the volume.

Specifications of Meshing of the geometry

air volume :

Elements : hex

Type : Cooper

Interval size : 0.5

Smooth the volume meshes by using the Length-weighted Laplacian Smoothing scheme. This scheme uses the average edge length of the elements surrounding each node.

Examining the mesh quality: The quality of mesh is assessed on the basis of skewness, which should not exceed 0.82.

Boundary conditions specified

Boundary conditions specify the flow and thermal variables on the boundaries of the physical model.

Wall : all the left side and right side faces , rear side face, all the interfaces (common faces of volumes), top and bottom faces of the geometrical model .

Symmetric : all the front side faces of the geometrical model .

Wall boundary conditions are used to bound fluid and solid zones. We can specify Fixed heat flux, Fixed temperature, Convective heat transfer, Combined external radiation and convection heat transfer thermal boundary conditions on Wall.

Symmetry boundary conditions are used when the physical geometry of interest, and the expected pattern of the flow / thermal insulation, have mirror symmetry.

Continuum specified

Fluid: volume of air inside room

Solid: All boundary walls

The generated meshed model is as shown in fig.4.4

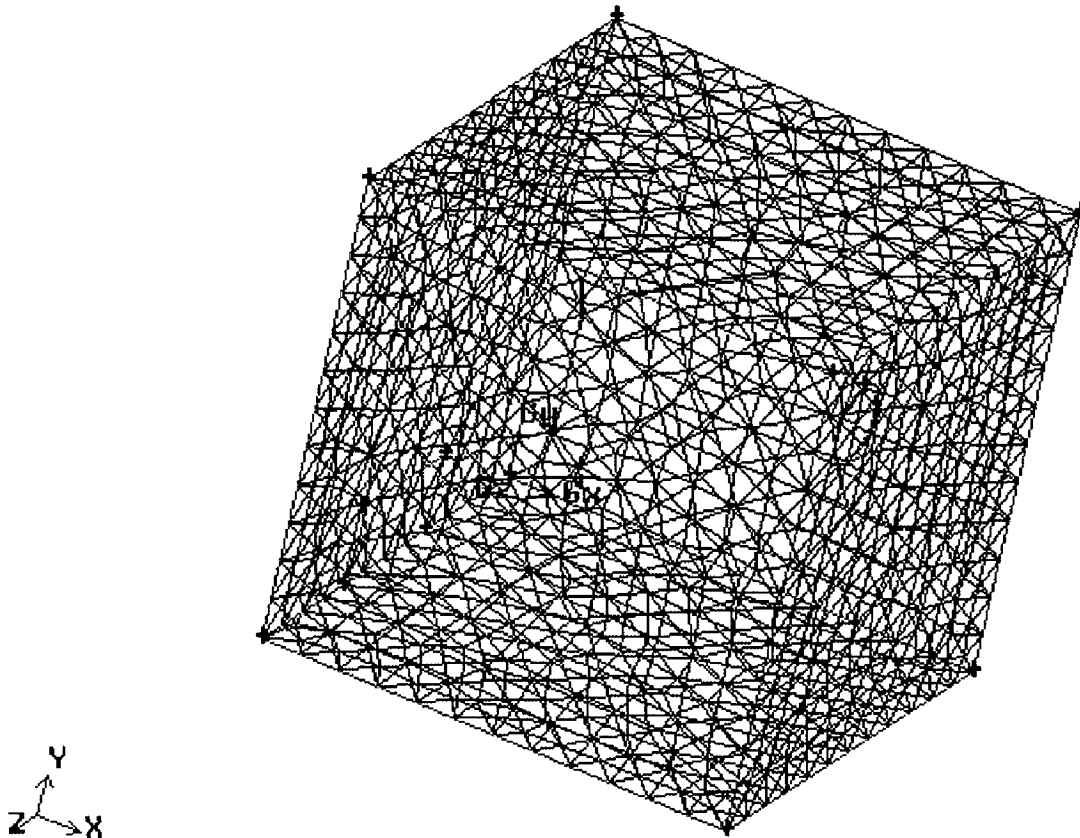


Fig. 4.4 Meshing geometry

ZONING:

In the created volume all the boundaries and inside volumes and inlets outlets are labeled.

The above figure 4.5 shows the labeled geometry.

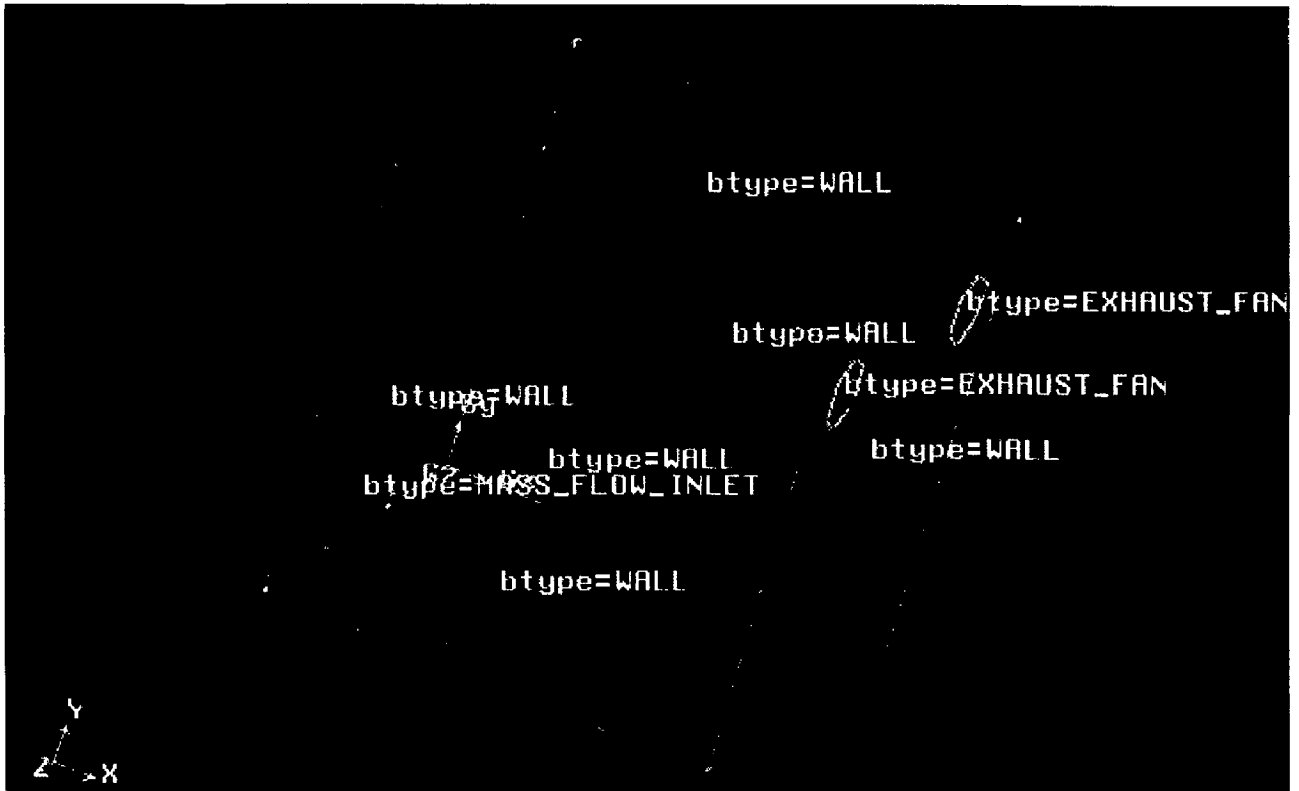


Fig 4.5 Labeled geometry

4.3 SOLUTION PROCESS

The mesh file is read in Fluent 6.2.16 solver. In solving the problem the following steps are involved.

Grid check, Grid scaling and Grid Display

After reading the mesh file, checking of grid and scaling of the grid is done. Grid can be seen through grid display panel.

Initial solution (Steady state) :

Numerical scheme choosen : Coupled

Coupled solver is the solution algorithm by which the governing equations are solved simultaneously.

Other models choosen : Energy

Viscous

Under viscous model, turbulent model is selected, because in this problem the flow field would be turbulent. Here three turbulent models are used. Results are displayed for the three turbulent models.

Specifying material properties :

For concrete and air the properties are taken from the FLUENT database.

Air properties are at normal temperature and pressure (atmospheric conditions):

Density	1.225	kg/m ³
Specific heat	1006.43	J/kg-K
Thermal conductivity	0.0242	W/m-K
Viscosity	0.00001789	kg/m-s

Concrete properties are at normal temperature and pressure (atmospheric conditions):

Density	2400	kg/m ³
Specific heat	885	J/kg-K
Thermal conductivity	242	W/m-K

Specifying operating conditions :

Operating pressure : 101325 pa

Gravity : -9.81 m/s²

Specifying boundary conditions

Here four types of boundary conditions are specified. Those are wall type, supply inlet, supply outlet, default interior.

In case of wall set the temperature of all walls at constant temperature normally at 300k. This is the main assumption for this model.

Wall thickness	0.25 m
Heat generation rate	0 W/m ³
Heat flux	0 W/m ²

In case of inlet the specification method is mass flow inlet.

Mass flow rate	1 kg/s
Total temperature at inlet	300K
Direction specification method	direction vector
Turbulent kinetic energy	$1\text{m}^2/\text{s}^2$
Turbulent dissipation rate	$1.2\text{ m}^2/\text{s}^3$

In case of the outlet air is sucked by exhaust fan

Gauge pressure	121590 Pascal
Back flow total temperature	300K
Turbulent specification method	k- ϵ model
Back flow turbulent kinetic energy	$1\text{ m}^2/\text{s}^2$
Target mass flow rate	1 kg/s

Discretization schemes chosen:

FLUENT uses a control-volume-based technique to convert the governing equations to algebraic equations that can be solved numerically.

Second-order Upwind Scheme gives the second order accuracy.

The discretization schemes chosen for governing equations are shown in below Table 4.1.

Table 4.1 :

Model	Discretization scheme
Flow	Second order upwind
Discrete ordinates	Second order upwind

Convergence criterion :

The convergence for the variables are defined in the following Table 4.2 .

Table 4.2 :

Variable	Convergence criterion
Continuity	0.001
X- velocity	0.001
Y- velocity	0.001
Z- velocity	0.001
Energy	1e-6

:

Solution Initialization and Iterations

Solution is initialized and iterations are carried out till the solution gets converged.

4.4 Development of Geometrical model 2

The problem is development of a room model of shape cube with proper inlets and outlets on the walls. In case of the **model 2** the inlet is an opening door on the side wall and outlets are exhaust fans on the opposite wall. In this case the temperatures of the walls are at different values.

Using proper commands of GAMBIT modeling, geometrical model (of physical model) has been developed.

The common faces (interfaces) of the volumes were connected.

The obtained model is as shown in the figure no 4.6

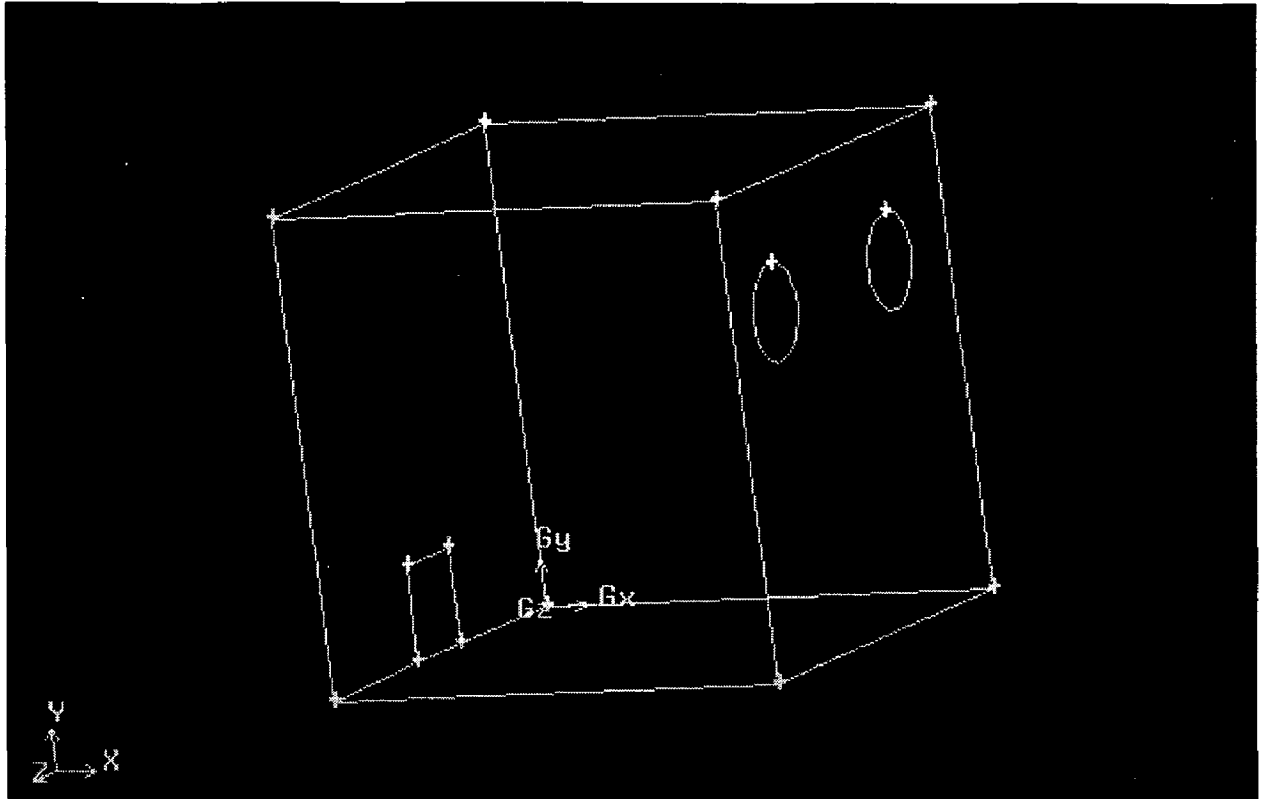


Fig.4.6 Isometric view

4.5 MESH GENERATION FOR MODEL 2

Meshing Scheme used:

Elements chosen : Hex

The Elements parameter defines the shape of the elements that are used to mesh the volume. Hex specifies that the mesh includes only hexahedral elements.

Type chosen : Cooper

The Type parameter defines the meshing algorithm and therefore, the overall pattern of mesh elements in the volume. Cooper algorithm sweeps the mesh node patterns of specified source faces through the volume.

Specifications of Meshing of the geometry

air volume :

Elements : hex

Type : cooper

Interval size : 0.5

Smooth the volume meshes by using the Length-weighted Laplacian Smoothing scheme. This scheme uses the average edge length of the elements surrounding each node.

Examining the mesh quality:The quality of mesh is assessed on the basis of skewness, which should not exceed 0.82.

Boundary conditions specified

Boundary conditions specify the flow and thermal variables on the boundaries of the physical model

Wall : all the leftside and right side faces , rear side face, all the interfaces (common faces of volumes), top and bottom faces of the geometrical model .

Symmetric : all the front side faces of the geometrical model .

Wall boundary conditions are used to bound fluid and solid zones. The temperatures of the walls are different .the inlet wall and ground wall at same temperature , front wall and back wall and side wall same temperature,top wall is at different temperature.

Symmetry boundary conditions are used when the physical geometry of interest, and the expected pattern of the flow / thermal insulation, have mirror symmetry.

Continuum specified

Fluid: volume of air inside room

Solid: All boundary walls

ZONING:

In the created volume all the boundaries and inside volumes and inlets outlets are labeled.

The following figure shows the labeled geometry

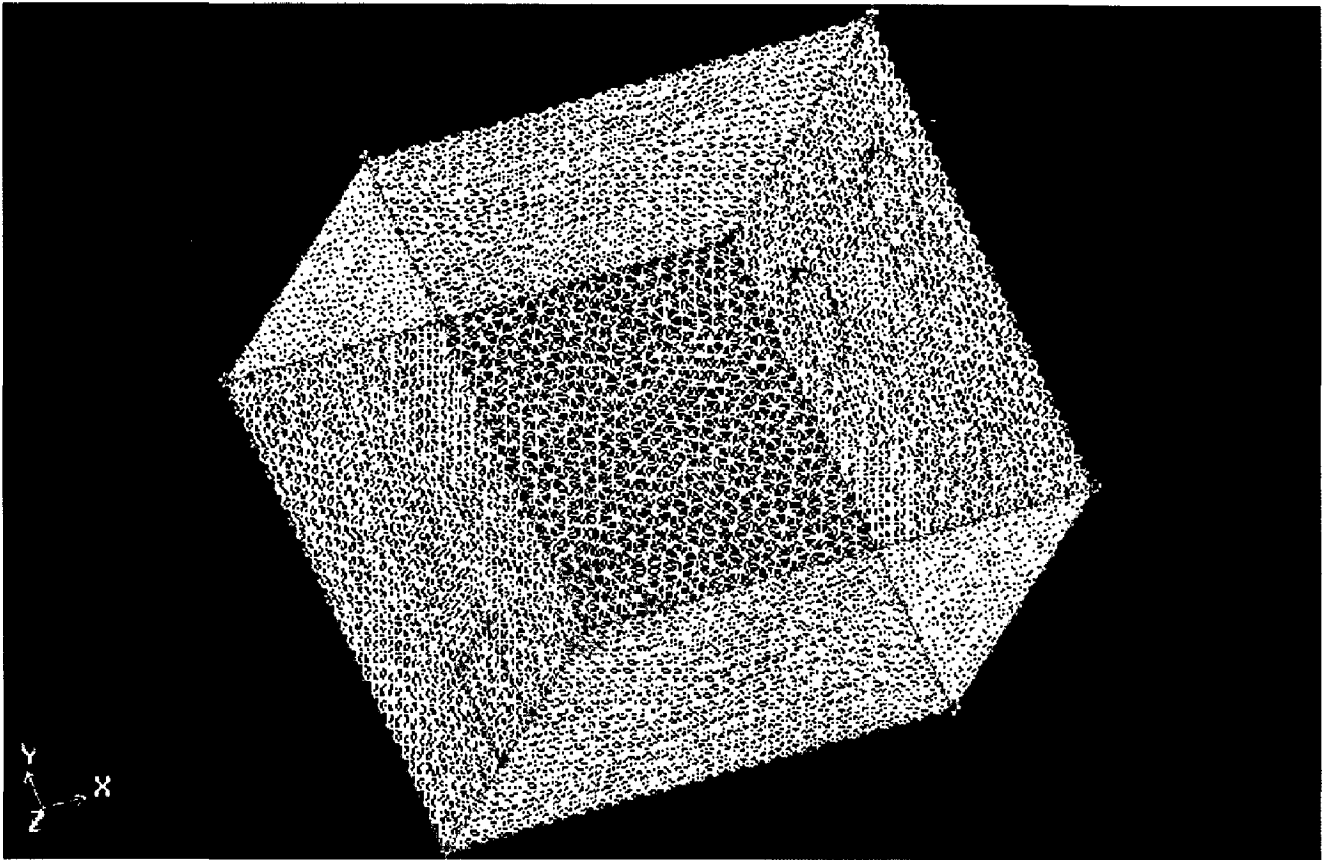


Fig.4.7 Meshing geometry

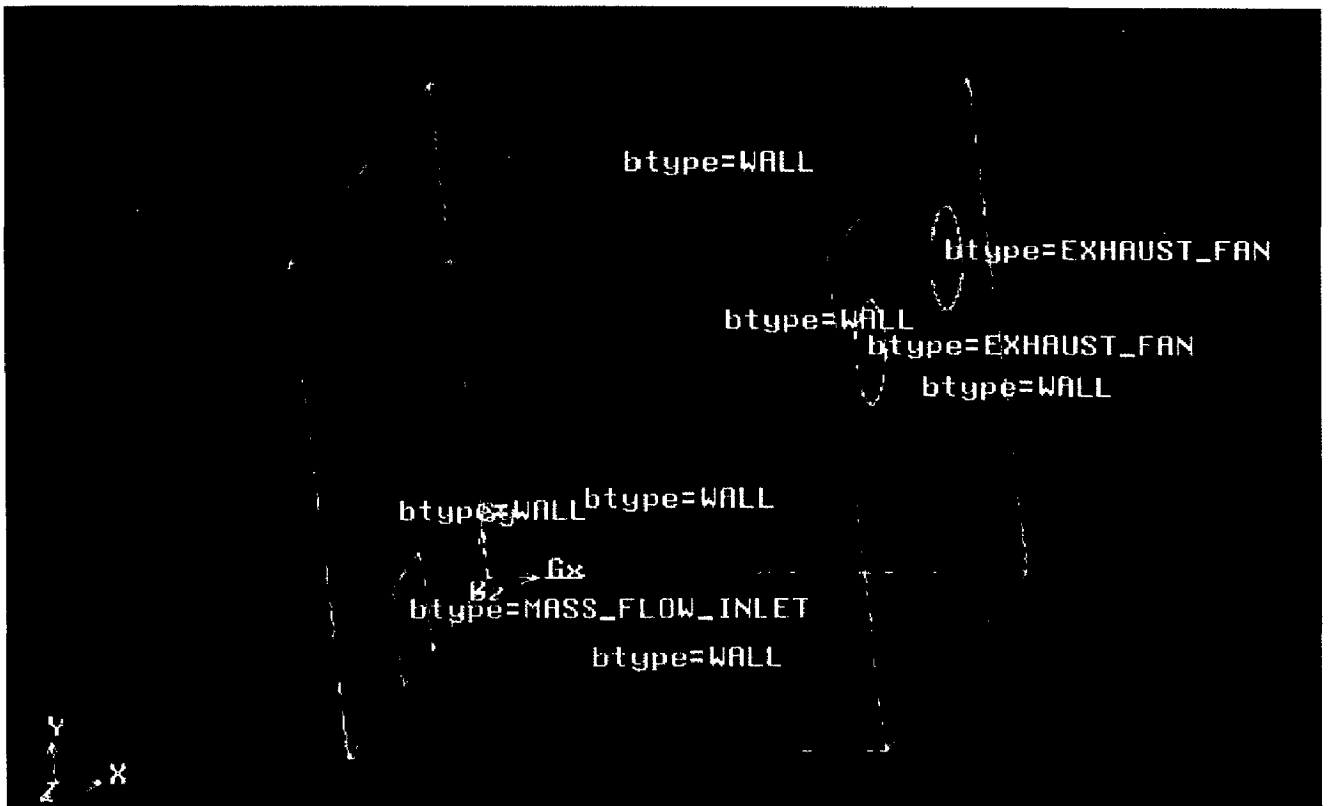


Fig.4.8 Labeled geometry

4.6 SOLUTION PROCESS

The mesh file is read in Fluent 6.2.16 solver. In solving the problem the following steps are involved.

Grid check, Grid scaling and Grid Display

After reading the mesh file, checking of grid and scaling of the grid is done. Grid can be seen through grid display panel.

Initial solution (Steady state) :

Numerical scheme choosen : Segregated

Segregated solver is the solution algorithm by which the governing equations are solved sequentially.(i.e., segregated from one another).

Other models choosen : Energy

Viscous

Under viscous model, turbulent model is selected, because in this problem the flow field would be turbulent. Here three turbulent models are used. Results are displayed for the three turbulent models.

Specifying material properties :

For concrete and air the properties taken from the FLUENT database as shown for model1.

Specifying operating conditions :

Operating pressure : 101325 pa

Gravity : -9.81 m/s²

Specifying boundary conditions

In case of wall set the temperature of all walls at different temperatures.

Inlet wall and ground wall temperature	303.15 K
Front wall temperature	313.15 K
Back wall temperature	313.15 K
Side wall temperature	313.15 K
Top wall temperature	318.15 K

The inlet and outlet boundary conditions are same as in the case of the **model 1**. discretization schemes and convergence criteria is also same as in the case of model 1.

Solution Initialization and Iterations

Initialize the solution and then do the iteration and after some iterations solution gets converged.

This section of the report deals with the results of the simulations carried for the different cases of room undertaken for study. Using the simulation technique described in chapter 4 and using the modeling equations as given in chapter 3, simulation is carried out with CFD package FLUENT 6.2.16 for ventilation in a room as described in chapter 4. Simulation was performed on P4 CPU based PC. To get the velocity profiles with in the room the geometry is meshed in gambit and then it is solved in fluent. The dimensions of the room are 6m*6m*6m. The velocity profiles and temperature profiles are discussed in following pages.

5.1 MODEL 1 RESULTS:

In case of model 1 the vectors of velocity and contours of velocity of air inside the room is important. The pressure distribution is same through out the room. Temperature of all walls is same and is also that of entering air at normal ambient temperature of 300K. So the temperature distribution is also constant. Hence, only velocity distribution is possible. In this case two turbulent models were used. These are k- ϵ model and Large Eddy Simulation.

5.1.1 Results from k- ϵ model

For the model 1 the convergence plot are shown in Fig 5.1 and Fig 5.2

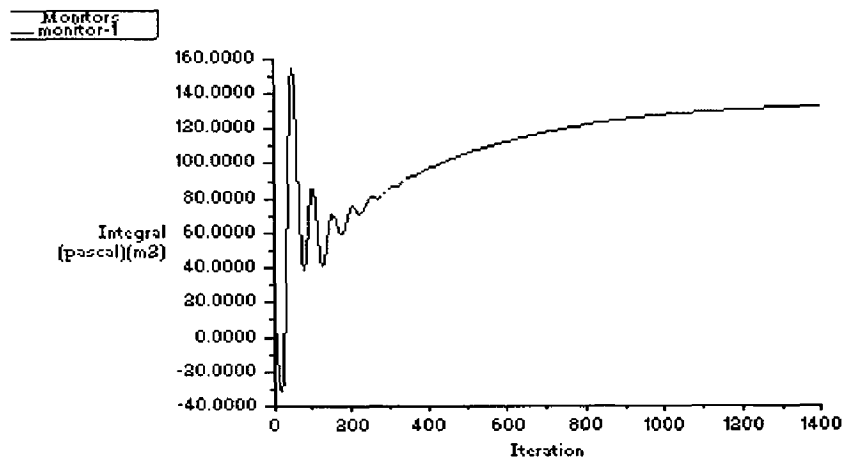


Fig.5.1 Convergence history of static pressure on boundary_type

From the convergence plots for the model 1 high computational work is required. The system is converged after the 1350 iterations.

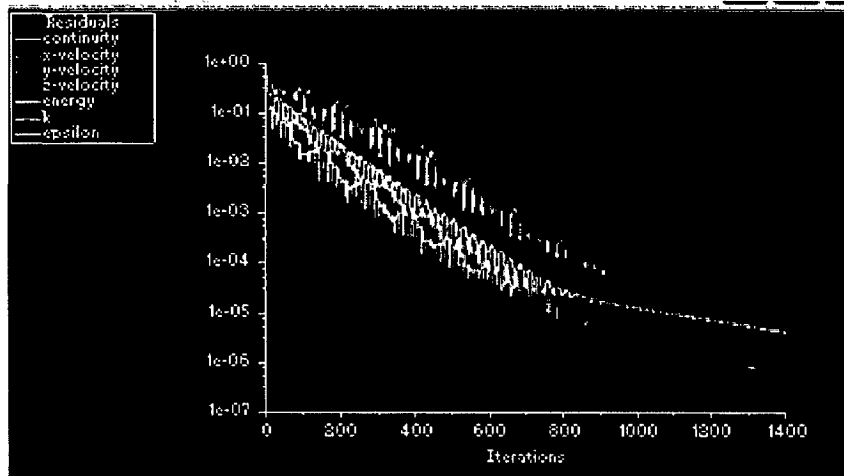


Fig.5.2 Scaled residuals

The grid display of the model 1 is shown in figure below

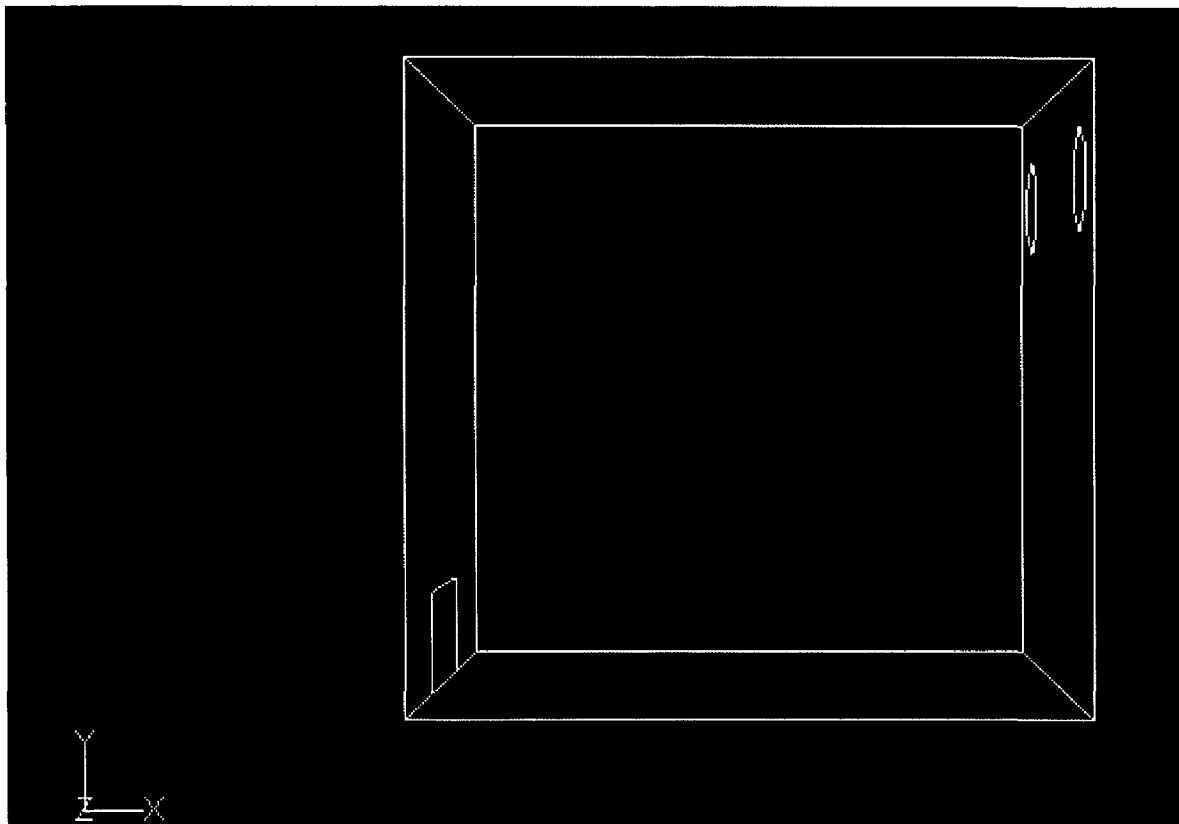


Fig.5.3 Grid display

The vector plots of air velocity at different iso surfaces and in default interior is shown in fig 5.5 to fig 5.8 at different x values of 1,3, 4 and 5 m. Where as fig 5.4 give three dimensional representation of air velocity inside the room.

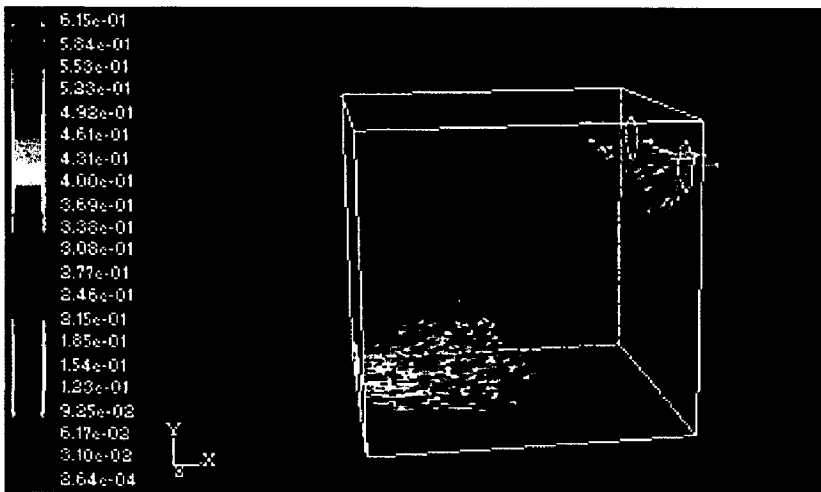


Fig.5.4 Velocity vectors colored by velocity magnitude (m/s)

From the fig 5.4 it can be shown that the air enters with high velocity. The remaining portion of the air is at low velocity and some air gets recirculated by the turbulent flow. As the air moving away from the inlet wall it moves like a jet and gets outward from the exhaust fans. There at outlets the air gets high velocity approximately in the range of 0.4 to the 0.6 m/s.

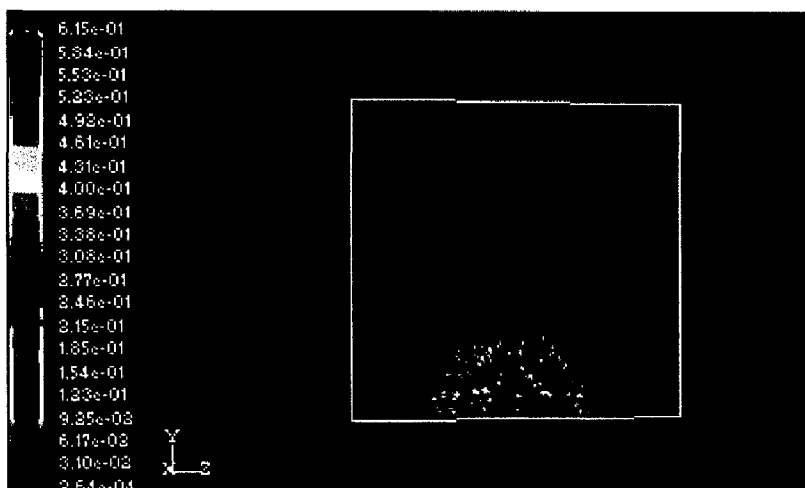
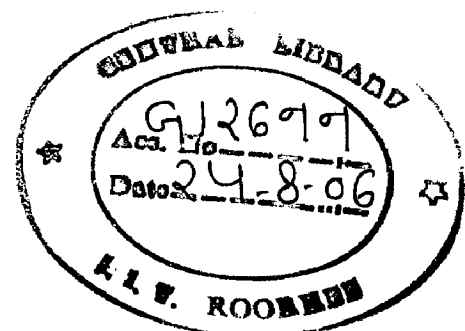


Fig.5.5 Velocity vectors colored by velocity magnitude (m/s) at x= 1m



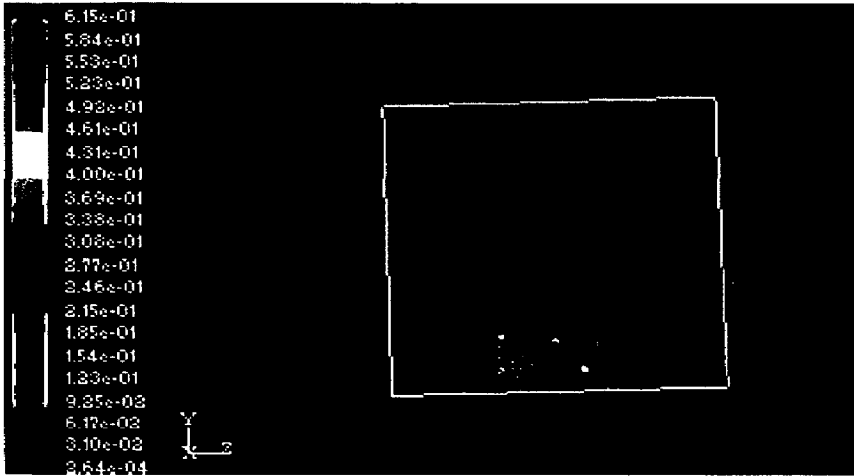


Fig.5.6 Velocity vectors colored by velocity magnitude (m/s) at $x= 3\text{m}$

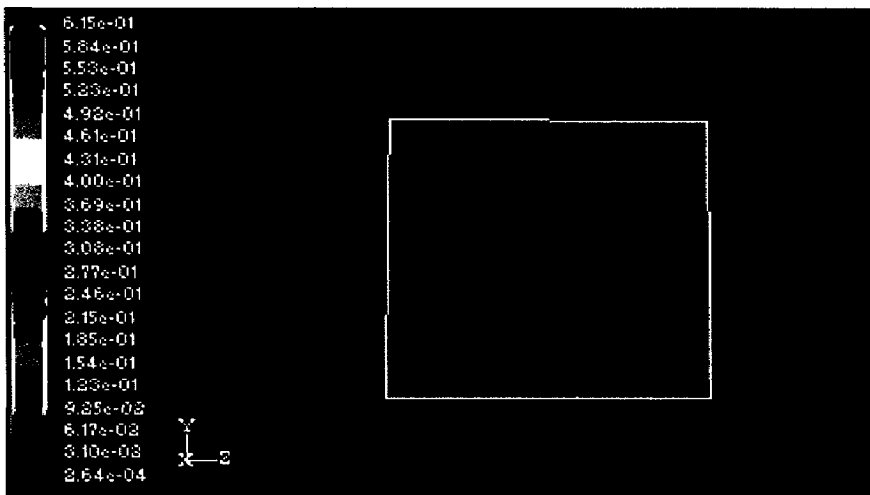


Fig.5.7 Velocity vectors colored by velocity magnitude (m/s) at $x= 4\text{m}$

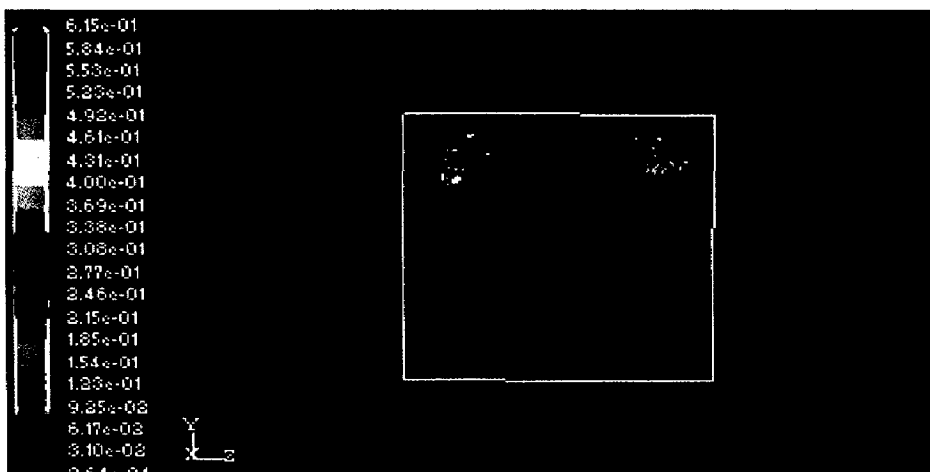


Fig.5.8 Velocity vectors colored by velocity magnitude (m/s) at $x= 5\text{m}$

Due to only two outlets placed on opposite wall to inlet air flow air flow is confined to near the inlet for $x=1\text{m}$ and slowly spreads and go up with increasing value of x and have higher velocities near the outlets for $x=5\text{m}$. Till $x=4\text{m}$, air flow is confined to central portion and will result in poor climate control. So finally from the velocity vectors at different position of x value it can be concluded that the air particles get low velocity as the moving away from inlet wall and gets more velocity at out let.

Contour plots of air velocity at different x locations are shown in fig 5.9 to fig 5.12.

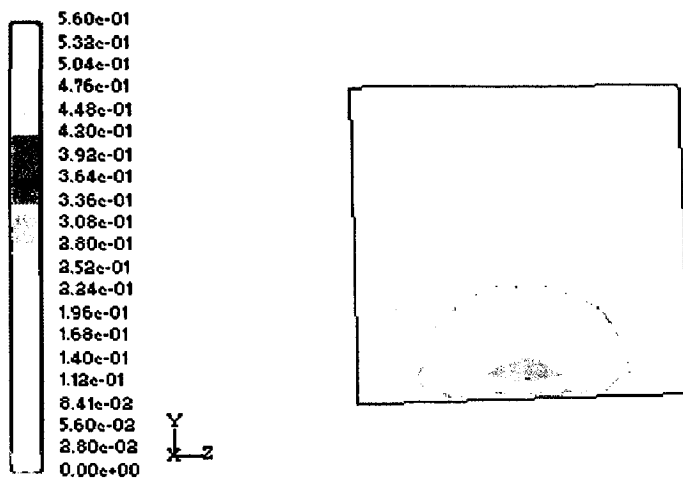


Fig.5.9 Contours of velocity magnitude (m/s) at $x=1\text{m}$

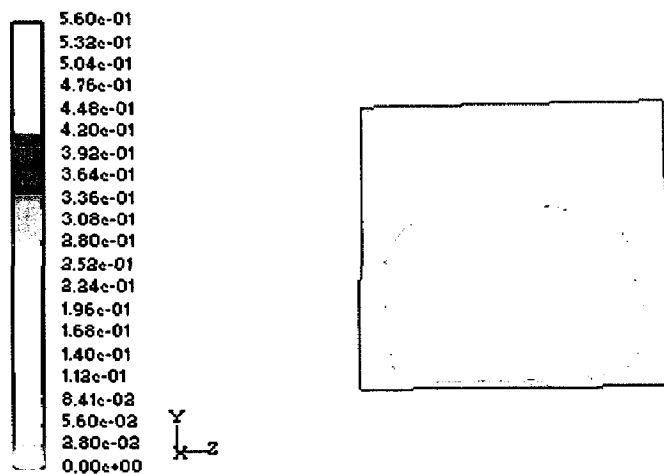


Fig.5.10 Contours of velocity magnitude (m/s) at $x=3\text{m}$

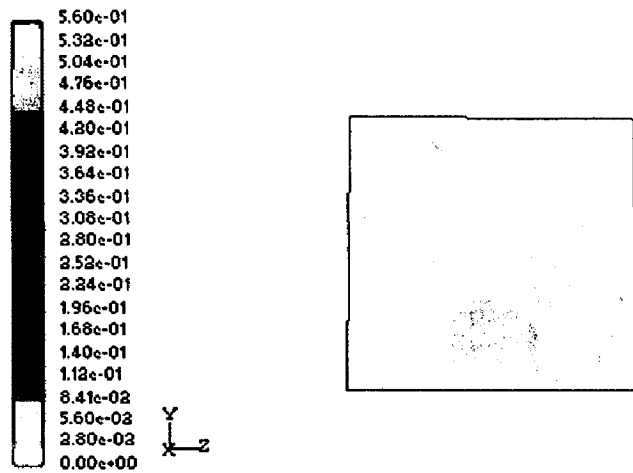


Fig.5.11 Contours of velocity magnitude (m/s) at $x=4\text{m}$

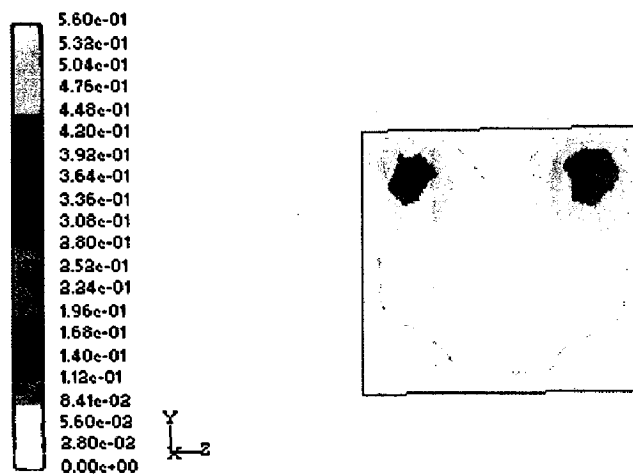


Fig.5.12 Contours of velocity magnitude (m/s) at $x=5\text{m}$

The information obtained in vector plots of air velocity from fig 5.4 to fig 5.8 is verified and displayed more widely in fig 5.9 to fig 5.12.

5.1.2 Results from Large Eddy simulation:

The model equations of LES model described in chapter 2. From the Eq (34) the velocity term and pressure terms are unknown variables. Those variables can get from the velocity distributions.

The convergence plot is shown in fig 5.13

The vector plots of air velocity by the Large Eddy Simulation are shown in figures 5.15 to fig 5.18.

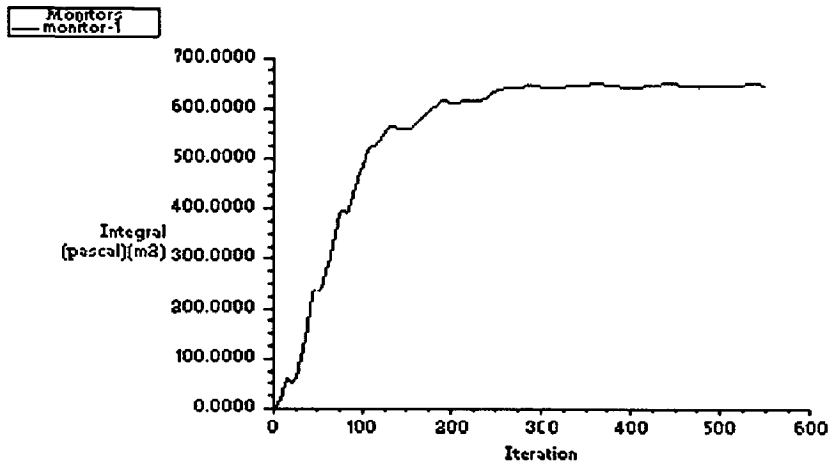


Fig.5.13 Convergence history of static pressure on boundary_type

In this case the system gets converged around 600 iterations. According to computational work needed for the convergence the LES model is the better. In case of two equation model more computational work is needed.

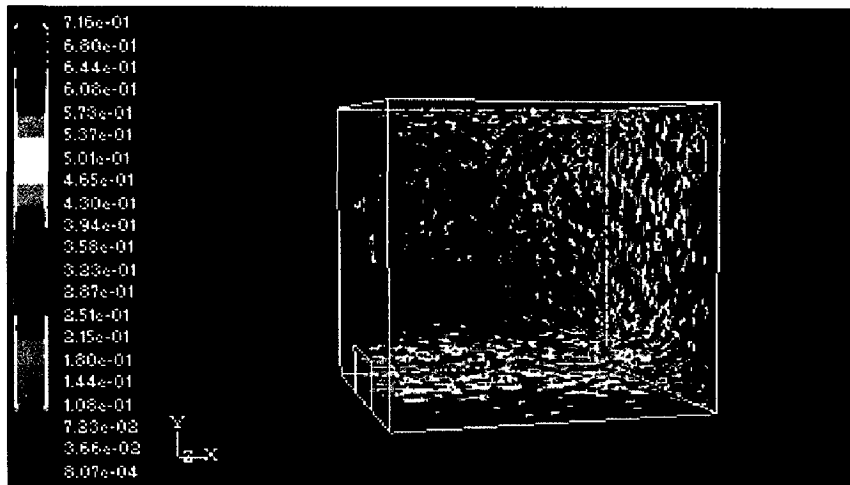


Fig 5.14 Velocity vectors colored by velocity magnitude (m/s)

From the fig 5.14 the air entering at high velocity at inlet then it moves like a jet up to at a distance $x=5m$ and then suddenly gets upward and in this direction it is coming back due to the eddy formation.

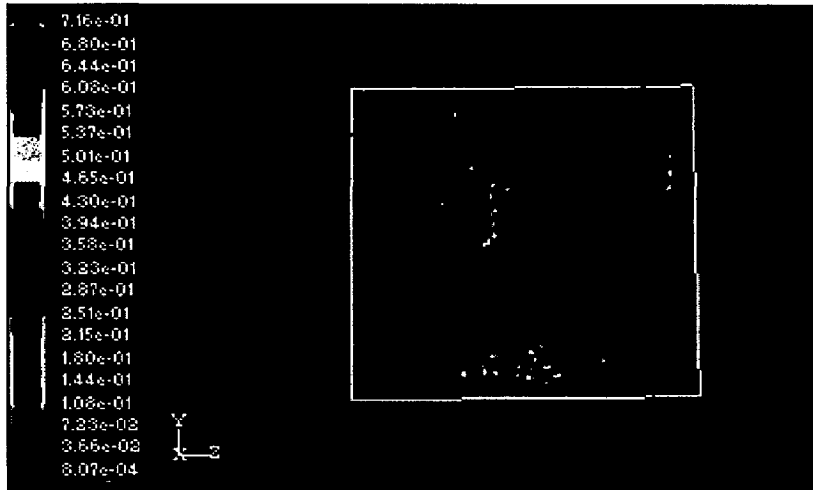


Fig.5.15 Velocity vectors colored by velocity magnitude (m/s) at $x=1\text{m}$

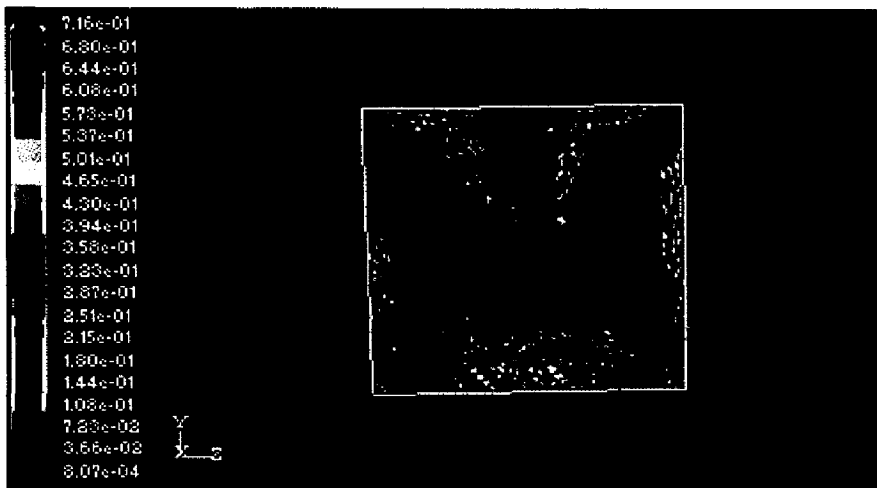


Fig.5.16 Velocity vectors colored by velocity magnitude (m/s) at $x=3\text{m}$

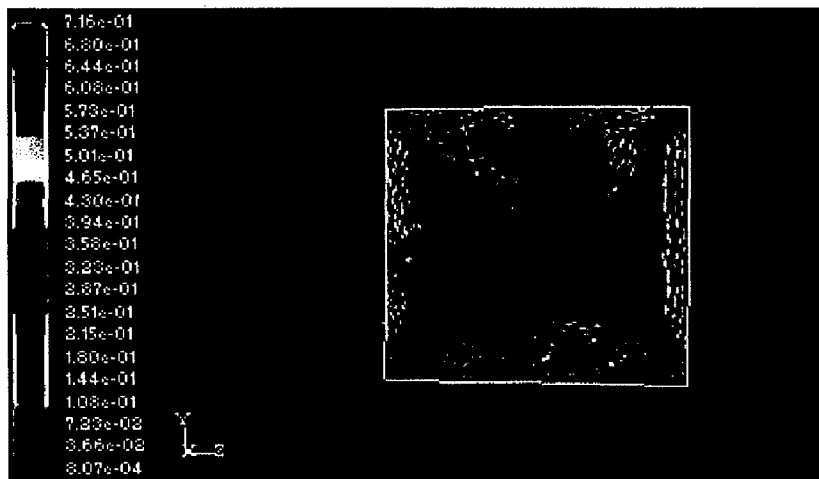


Fig.5.17 Velocity vectors colored by velocity magnitude (m/s) at $x=4\text{m}$

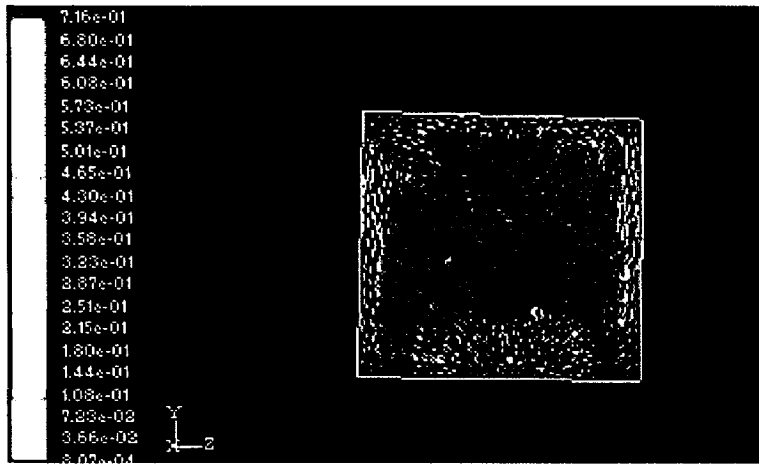


Fig.5.18 Velocity vectors colored by velocity magnitude (m/s)
at $x=5m$

In these figures from 5.14 to 5.18 the air particles near by the walls get more velocity as the distance from the inlet wall increases. From the above two turbulent model results it can be concluded that the two equation model gives more realistic representation of air flow with in the room. As the air moving up wards it is not spreading through out the room due to the turbulence. The person besides the walls of the room can't get the proper fresh air. So more number of inlets has to be provided for the proper atmosphere with in the room and more number of outlets are also to be provided for proper ventilation system.

5.2 MODEL 2 RESULTS:

In the model 2 the room dimensions are 6m width, 6m long and 6m height. The inlet door is on the side wall. The dimensions of inlet are 2m width and 1m height. The side wall and bottom wall at same temperature and roof is at high temperature. Convergence plots are shown in fig 5.19 and fig 5.20. This model is converged around 478 iterations.

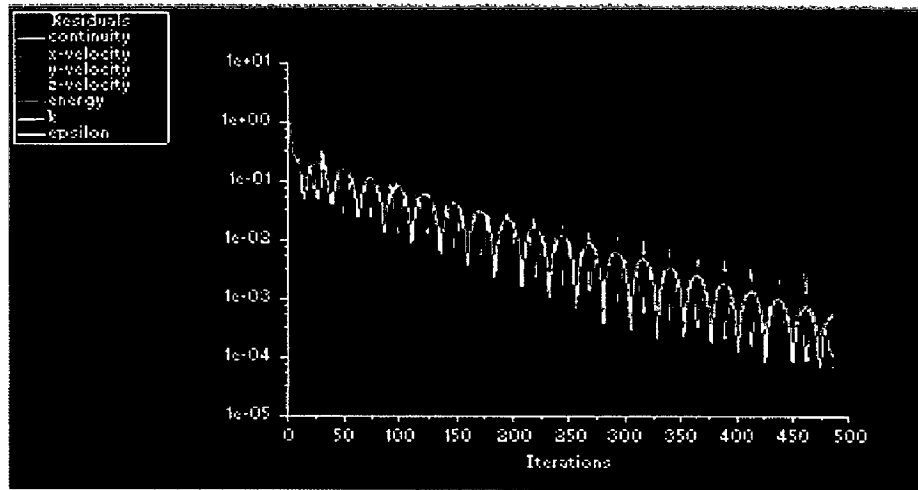


Fig 5.19 Scaled residuals

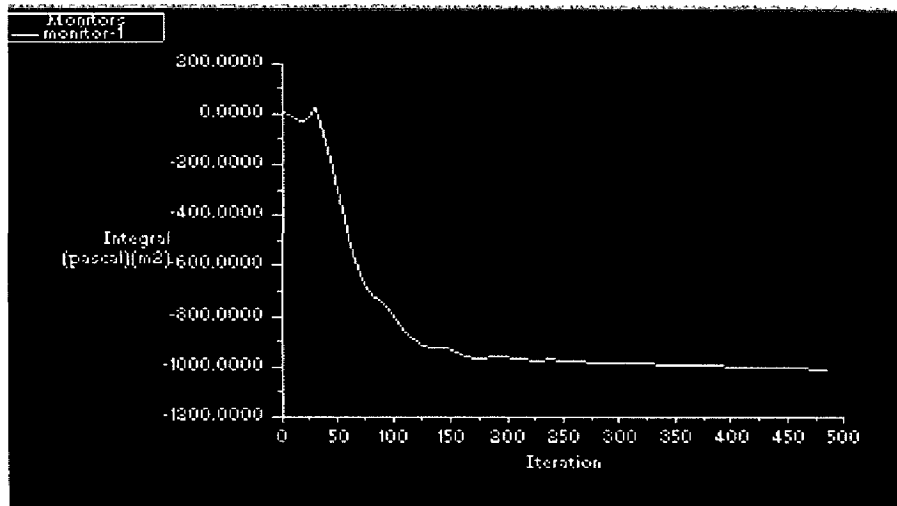


Fig 5.20 Convergence history of static pressure on Default interior

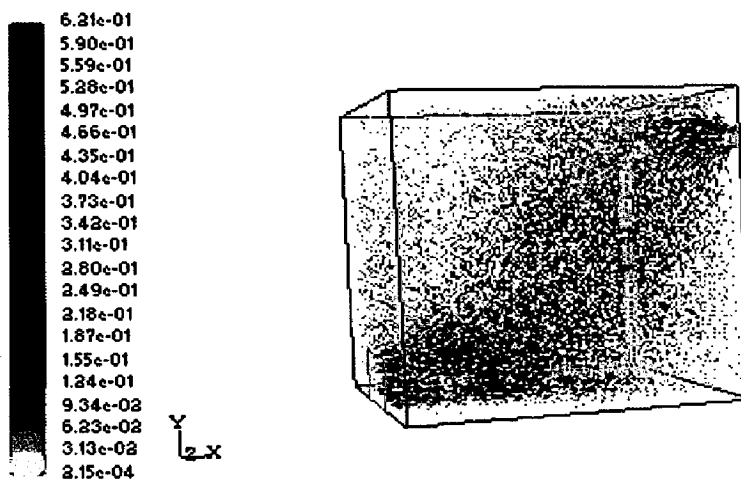


Fig 5.21 Velocity vectors colored by velocity magnitude (m/s)

From the fig 5.21 the air particles entering at inlet has high velocity. The walls are at high temperature so the air particles move upward and recirculated by turbulent flow. The region besides the wall is not occupied by the fresh air. The air coming from inlet moves as a jet and gets upward as in the case of model1. So for better air circulation more number of inlets is to be provided.

The Temperature profiles shown in fig 5.22 to fig 5.25.

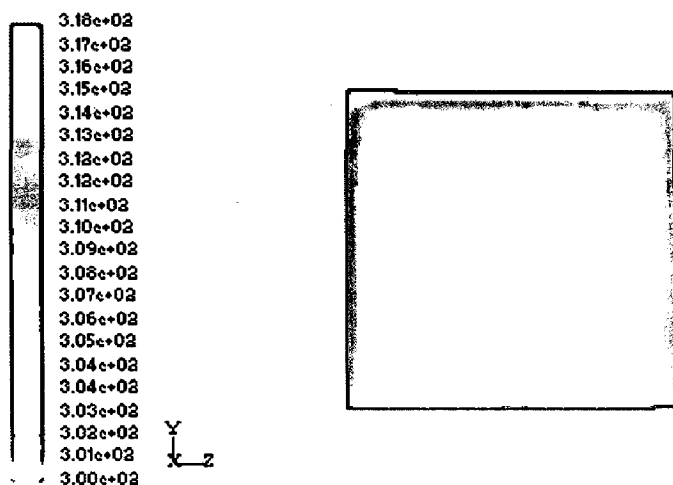


Fig.5.22 Contours of static temperature (K) at x=1m

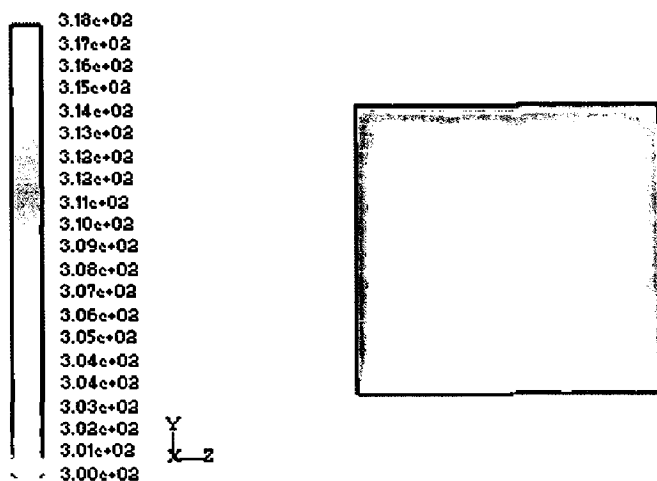


Fig.5.23 Contours of static temperature (K) at x=3m

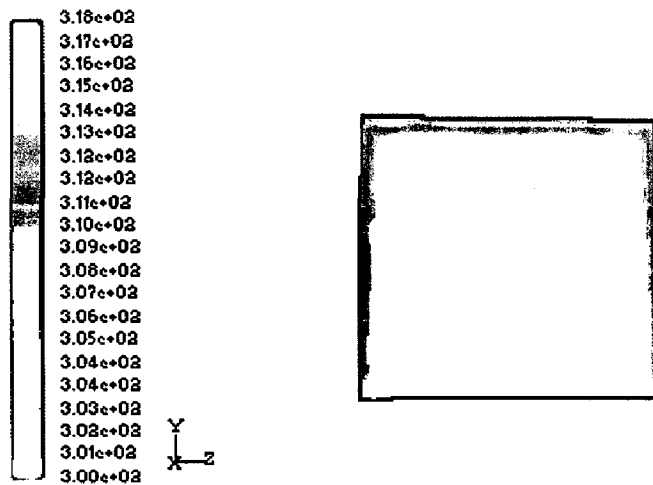


Fig.5.24 Contours of static temperature (K) at x=4m

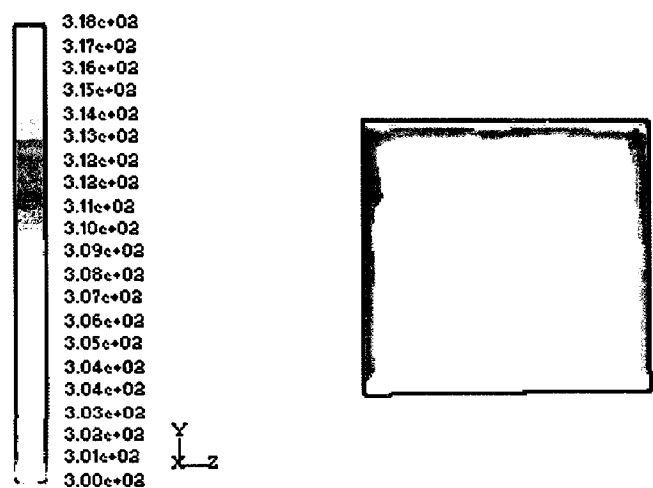


Fig.5.25 Contours of static temperature (K) at x=5m

From the temperature profiles the temperature of the air beside the wall is very high. The roof is the high temperature wall which is maintained at 318.15K. The surrounding air has got up to 312K to 316K. The air enters at 300K. From the profiles at x=1m the low temperature air region is more at inlet. As moving away from wall the air gets high temperature, the low temperature region gets decreases as x reaches to 4m. At x= 5m plane the minimum temperature is nearly 305K. By creating the point surface with in the Default interior the temperature at any point with in the room cane be measured directly.

The vector plots of air velocity is shown in fig 5.26 to 5.29.

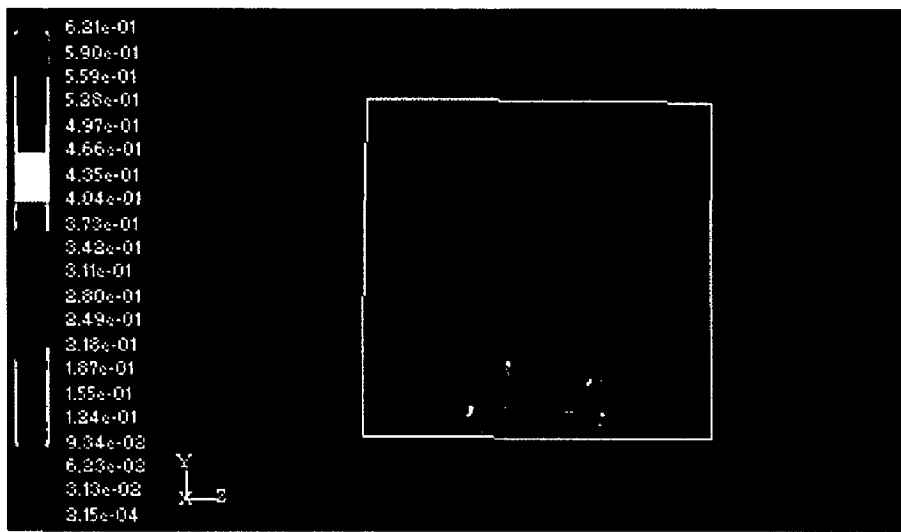


Fig 5.26 Velocity vectors colored by velocity magnitude (m/s) at $x=1\text{m}$

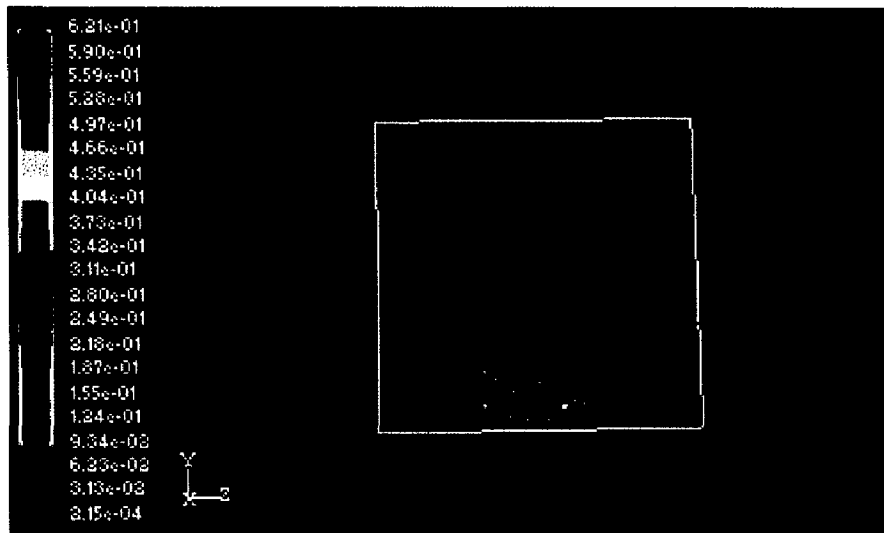


Fig 5.27 Velocity vectors colored by velocity magnitude (m/s) at $x=3\text{m}$

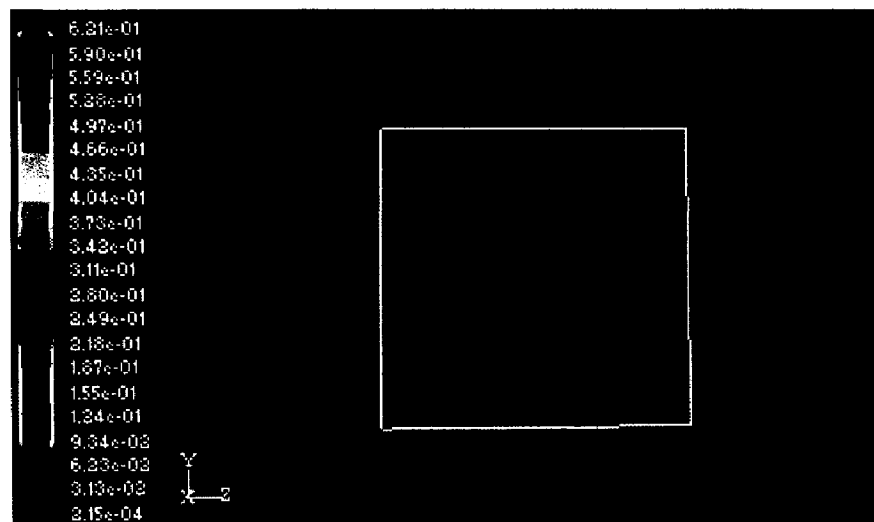


Fig 5.28 Velocity vectors colored by velocity magnitude (m/s) at $x=4\text{m}$

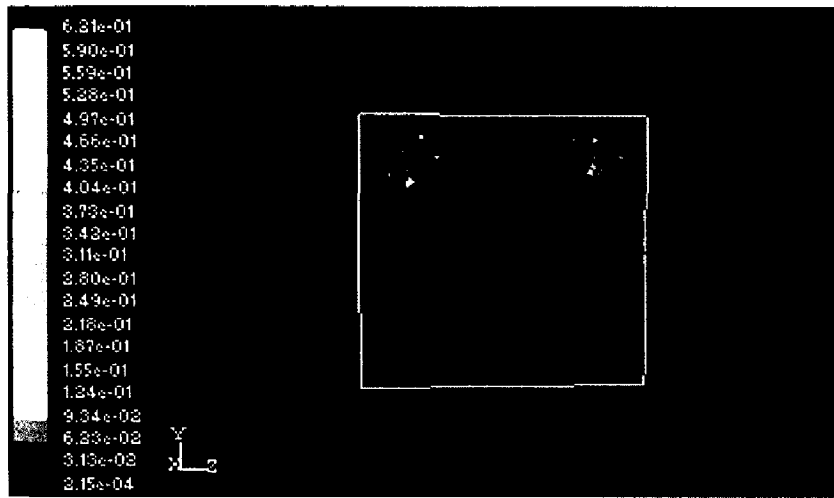


Fig 5.29 Velocity vectors colored by velocity magnitude (m/s) at $x=5\text{m}$

From the above vectors plots the velocity of air at entering is more and moves with in a room as a jet and go upward and gets high velocity at outlet. These plots are same as in the case of the model1. The heating effect of the walls on the air particle velocity is not that much large. Due to heating the air gets slight high velocity comparatively to the case of model1. At the outlet the velocity of air is nearly 0.405m/s.

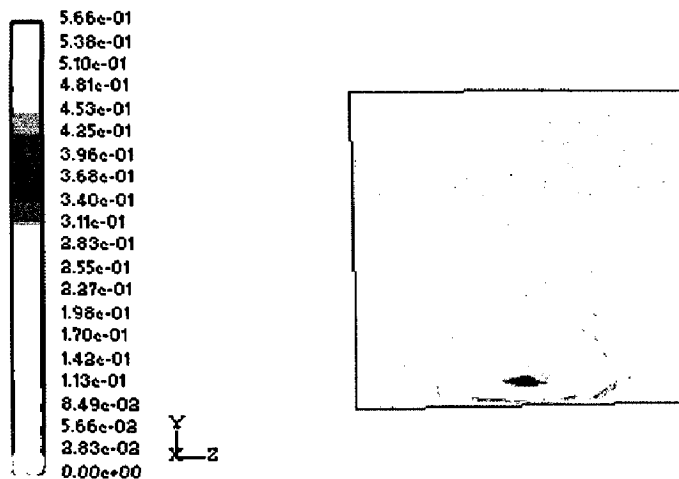


Fig.5.30 Contours of velocity magnitude (m/s) at $x= 1\text{m}$

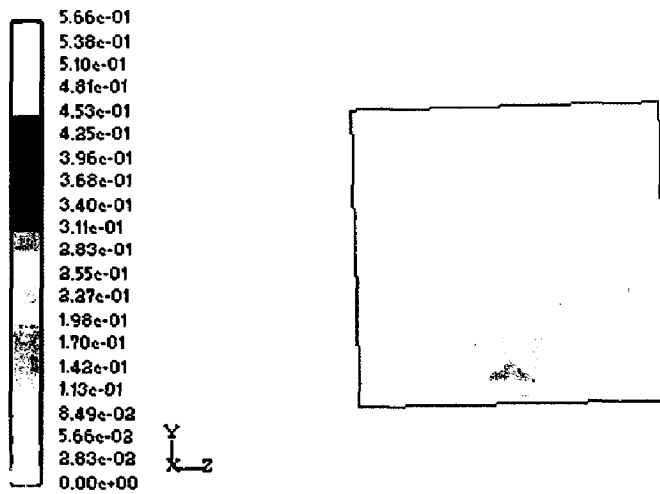


Fig.5.31 Contours of velocity magnitude (m/s) at $x=3m$

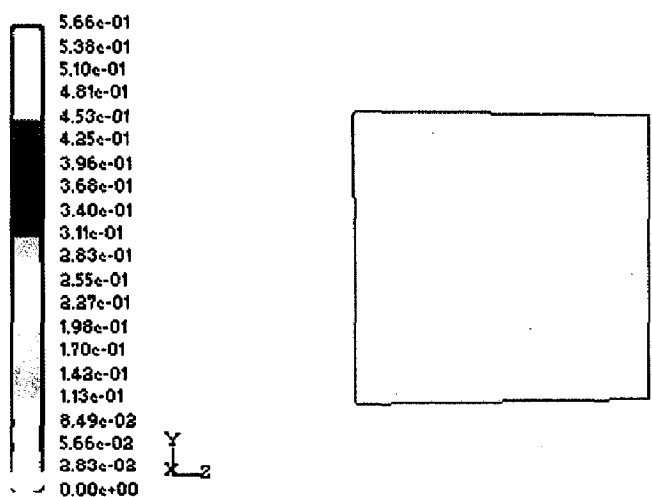


Fig.5.32 Contours of velocity magnitude (m/s) at $x=4m$

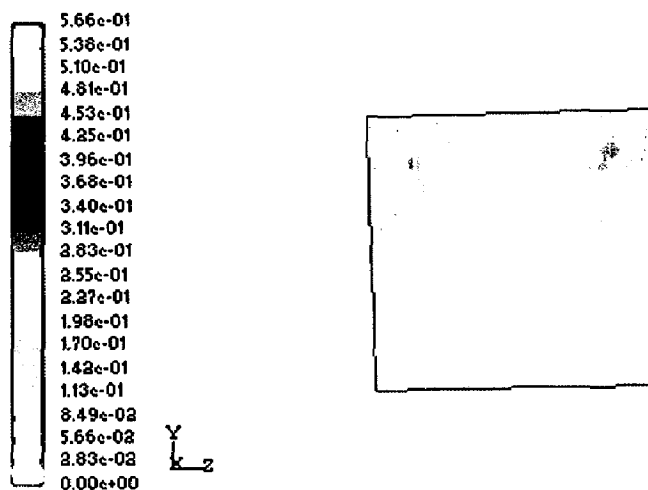


Fig.5.33 Contours of velocity magnitude (m/s) at $x=5m$

The information obtained in vector plots of air velocity from fig 5.26 to fig 5.29 is verified and displayed more widely in fig 5.30 to fig 5.33.

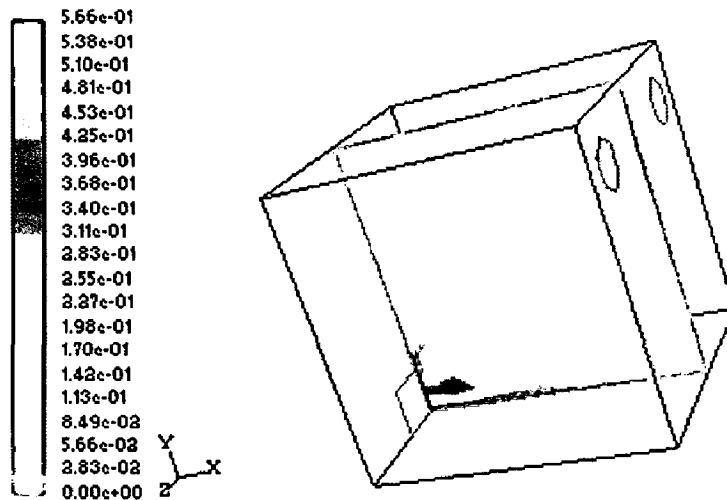


Fig.5.34 Contours of velocity magnitude (m/s) at $z= 5\text{m}$

In the fig 5.34 the contours of velocity are shown .It can be conclude that the air entered gets recirculated on that plane up to the $x=5\text{m}$, after that it is not coming back. Like this the contours of air velocity can be shown on any plane in any direction.

It is confirmed that numerical simulation of the velocity and thermal and diffusion fields in a conventional flow type of clean room is very useful in comprehending flow and diffusion patterns. The developments in mathematical and numerical modelling of turbulent flows in theory allow an improved simulation of the indoor air flow problem with Computational Fluid Dynamics (CFD). Validation of these models however remains an issue of concern given the indoor air flow characteristics and the limited number of validation studies for realistic indoor air flow patterns to evaluate the improved models. Nonetheless, CFD has taken a prominent position in the indoor climate research.

CFD based softwares are more useful for temperature distribution and pressure distribution and velocity distribution. It also gives the good comparison between the turbulent models, i.e which turbulent model applicable to particular room ventilation.

The wall heat transfer characteristics are not correctly predicted with logarithmic wall functions unless rigid control on the y^+ -value is executed (in the order of ± 1) and therewith on the near-wall grid distribution. The law-of-the-wall is not valid for the type of boundary layer flows that appear indoors. Correcting the wall heat transfer characteristics by imposing convection heat transfer data improves the agreement between measured and simulated temperature distribution and flow pattern. The use of low-Reynolds number turbulence models to solve the boundary layer flow up to the wall currently does not represent an alternative, given the high computer capacity requirements to model an indoor air flow configuration. The in this work derived measurement data can be used to validate new wall functions or empirical relations.

The two turbulent models two-equation model and Large Eddy Simulation are compared. The Two equation model gave the more realistic approach comparatively than LES model. But for the two-equation model more intensive computational work is required

FUTURE WORK:

In this project the velocity profiles and temperature profiles of different room models are studied. In future the work can be extended to the study of temperature profiles with the heat generation within the room and heat flux through walls. Unsteady states can be studied for sudden emission of pollutants/contaminants and/or energy release. In this project the simulation is carried out using only one CFD package namely, Fluent software, for comparison simulation runs can also be carried out using other CFD packages like Phoenics and CFX etc. At present, only turbulence models have been used to study velocity profiles, this can be extended to include other turbulent models for comparison and better understanding of air flow inside a room.

NOMENCLATURE:

g_i, g_j, g_k	Tensor notation for gravitational acceleration	(m/s ²)
h	Enthalpy	(J/kg)
K	Thermal conductivity	(W/(m.K))
k	Turbulent kinetic energy	(m ² /s ²)
k_{in}	Turbulent energy at room inlet	(m ² /s ²)
$k_{i,j,k}$	Turbulent energy at cell (i,j,k)	(m ² /s ²)
t	Time	(s)
x_i, x_j, x_k	Tensor notation for principle directions	
x_n	Normal direction	
q''	Heat flux vector	(J/(m ² .s))
u', v', w'	Velocity fluctuations in x, y, and z-directions	(m/s)
y_n	Normal distance	(m)
A	Generic property	
A_{in}, A_{out}	Inlet and outlet cross-sectional areas	(m ²)
C_p	Specific heat	(J/(kg.K))
C_μ, C_1, C_2	Constants for the k- ϵ model	
D	Mass divergence	(1/s)
F_μ, F_1, F_2, E	Empirical functions for the k- ϵ model	
P	Pressure	(Pa)
$P_{i,j,k}$	Pressure at cell (i,j,k)	(Pa)
R_τ	Turbulent Reynolds number	
R_y	Local Reynolds number	
T	Temperature	(K)
T_0	Reference temperature	(K)
$T_{i,j,k}$	Temperature at cell (i,j,k)	(K)
U, V, W	Velocity components in x, y, and z-directions	(m/s)
U_{jet}	Inlet velocity	(m/s)

U_n	Normal Velocity	(m/s)
U_{out}	Outlet velocity	(m/s)
U_t	Tangential velocity	(m/s)
U_i, U_j, U_k	Tensor notation for velocity components	(m/s)
U_i, V_i, W_i	Tensor notation for mean velocity components	(m/s)
$U_{i,j,k}$	U velocity at cell (i,j,k)	(m/s)
$V_{i,j,k}$	V velocity at cell (i,j,k)	(m/s)
α	Thermal diffusivity	(m ² /s)
β	Thermal expansion coefficient	(1/K)
ε	Turbulent energy dissipation rate	(m ² /s ³)
$\varepsilon_{i,j,k}$	Turbulence dissipation rate at cell (i,j,k)	(m ² /s ³)
ε_{in}	Turbulent dissipation rate at room inlet	(m ² /s ³)
ρ	Density	(kg/m ³)
μ	Dynamic viscosity	(kg/(m.s))
ν	Kinematic viscosity	(m ² /s)
ν_t	Turbulent viscosity	(m ² /s)

REFERENCES

1. Awbi, H.B., "Application of Computational Fluid Dynamics in Room Ventilation." *Building and Environment*. Vol. 24, No. 1. (1989)
2. Baker, A.J. and R.M. Kelso, "On Validation of Computational Fluid Dynamics Procedures for Room Air Motion Prediction." *ASHRAE Transactions*. Vol. 96, No. 1(1990)
3. Chen, Q., A. Moser, and A. Huber, "Prediction of Buoyant, Turbulent Flow by a low-Reynolds Number $k-\varepsilon$ Model." *ASHRAE Transactions*. Vol. 96, Pt. 1. (1990)
4. Gosman, A.D., P.V. Nielsen, A. Restivo, and J.H. Whitelaw, "The Flow Properties of Rooms with Small Ventilation Openings." *Journal of Fluids Engineering*. Vol. 102. (1980)
5. Harlow, F.H. and J.E. Welch, "Numerical Calculation of Time-Dependent Viscous Incompressible Flow of Fluid with Free-Surface." *The Physics of Fluids*. Vol. 8, No. 13. (1965)
6. Hinze, J.O., *Turbulence* (2nd Edition). McGraw-Hill. New York. (1987)
7. Hirt, C.W. and J.L. Cook, "Calculating Three-Dimensional Flows Around Structures and over Rough Terrain." *Journal of Computational Physics*. Vol. 10. (1972)

8. Hirt, C.W., B.D. Nichols, and N.C. Romero, "SOLA - A Numerical Solution Algorithm for Transient Fluid Flows." Report LA-5852, Los Alamos Scientific Laboratory. (1975)
9. Lam, C.G. and K. Bremhorst, "A Modified Form of the $k-\varepsilon$ Model for Predicting Wall Turbulence." ASME Transactions. Vol. 103. (1981)
10. Launder, B.E. and D.B. Spalding, "The Numerical Computation of Turbulent Flows." Computer Methods in Applied Mechanics and Engineering. Vol. 3. (1974)
11. Lilley, D.G., "Three-Dimensional Flow Prediction for Industrial Mixing." ASME International Computers in Engineering Conference. (1988)
12. Murakami, S., S. Kato, and Y. Suyama, "Three-Dimensional Numerical Simulation of Turbulent Airflow in a Ventilated Room by Means of a Two-Equation Model." ASHRAE Transactions. Vol. 93, Pt. 2. (1987)
13. Murakami S. and S. Kato, "Numerical and Experimental Study on Room Airflow. 3-D Predictions using the $k-\varepsilon$ Turbulence Model." Building and Environment. Vol. 24, No. 1. (1989a)
14. Murakami, S., S. Kato, and Y. Suyama, "Numerical Study on Diffusion Field as Affected by Arrangement of Supply and Exhaust Openings in Conventional-Flow-Type Clean Room." ASHRAE Transactions. Vol. 95, Pt. 2. (1989b)
15. Murakami, S., S. Kato, and Y. Ishida, "3-D Numerical Simulation of Turbulent Air Flow in and Around Buildings Based on the $k-\varepsilon$ Model with Generalized Curvilinear Coordinates." ASHRAE Transactions. Vol. 95, Pt. 2. (1989c)

16. Murakami, S., S. Kato, and Y. Suyama, "Numerical Study of Flow and Contaminant Diffusion Fields as Affected by Flow Obstacles in Conventional-Flow-Type Clean Room." ASHRAE Transactions. Vol. 96, Pt. 2. (1990)
17. Nielsen, P.V., A. Restivo, and J.H. Whitelaw, "The Velocity Characteristics of Ventilated Rooms." Journal of Fluids Engineering. Vol. 100. (1978)
18. Patel, V.C., W. Rodi, and G. Scheurer, "Turbulent Models for Near-Wall and low-Reynolds Number Flows: A Review." AIAA Journal. Vol. 23, No. 9. (1984)
19. Prasad, K.K., *Introduction to turbulent flows*, lecture notes, Eindhoven University of Technology, Eindhoven, The Netherlands. (1994)
20. Rodi, W., "Turbulence Models for Environmental Problems." Prediction Methods for Turbulent Flows. W. Kollman, ed. Hemisphere/McGraw-Hill. New York. (1980)
21. Shih, T.M., Numerical Heat Transfer. Hemisphere Publishing Company. New York. (1984)
22. Spitler, J.D., "An Experimental Investigation of Air Flow and Convective Heat Transfer in Enclosures Having Large Ventilative Rates." Ph.D. Thesis. Department of Mechanical and Industrial Engineering, University of Illinois at Urbana-Champaign. (1990)
23. Spitler, J.D., C.O. Pederson, D.E. Fisher, P.F. Menne, and J. Cantillo, "An Experimental Facility for Investigation of Interior Convective Heat Transfer." ASHRAE Transactions. Vol. 97, Pt. 1. (1991)

24. Tavoularis, S., Techniques for turbulence measurement, In: *Encyclopedia of Fluid Mechanics, volume 1: Flow Phenomena and Measurement* (ed: N.P. Cheremisinoff), Chapter 36, Gulf Publishing Company, Houston, USA. (1986)

25. Williams, P.T., Baker, A.J. and Kelso, R.M., Numerical calculation of room air motion - part 2: The continuity constraint finite element method for three-dimensional incompressible thermal flows, *ASHRAE Transactions*, vol.100 part 1, pp.531-548. (1994)